

**DETERMINATION OF AN IMPROVED SPECTRUM SENSING THRESHOLD FOR
COGNITIVE RADIO USING SMOOTHED PSEUDO
WIGNER-VILLE DISTRIBUTION**

BY

Wasiu Olayinka AJADI

P14EGCP8005

hajardy@gmail.com

Supervisory Committee

Dr. S. M. Sani (Chairman)

Dr. A.M.S. Tekanyi (Member)

**A Dissertation Submitted to the Department of Electrical and Computer Engineering,
Ahmadu Bello University, Zaria in Partial Fulfillment of the Requirements for the Award
of Master of Science (M.Sc.) Degree in Telecommunications Engineering**

March, 2017

DECLARATION

I AJADI Wasiu Olayinka, hereby declare that the work in this dissertation entitled “Determination of an Improved Spectrum Sensing Threshold for Cognitive Radio Using Smoothed Pseudo Wigner-Ville Distribution” has been carried out by me in the Department of Electrical and Computer Engineering. The information derived from literature has been duly acknowledged in the text and a list of references provided. No part of this dissertation was previously presented for another degree or diploma at this or any other institution.

Ajadi Wasiu Olayinka

Signature

Date

CERTIFICATION

This Dissertation entitled **“DETERMINATION OF AN IMPROVED SPECTRUM SENSING THRESHOLD FOR COGNITIVE RADIO USING SMOOTHED PSEUDO WIGNER-VILLE DISTRIBUTION”** by WasIU Olayinka AJADI meets the regulations governing the award of degree of Master of Science (MSc) in Telecommunications Engineering of the Ahmadu Bello University, and is approved for its contribution to knowledge and literary presentation.

Dr. S. M. Sani
Chairman, Supervisory Committee

(Signature) Date _____

Dr. A. M. S. Tekanyi
Member, Supervisory Committee

(Signature) Date _____

Dr. Y. Jibril
Head of Department

(Signature) Date _____

Prof. S. Z. Abubakar
Dean. School of Postgraduate Studies

(Signature) Date _____

DEDICATION

This research work is dedicated to Almighty ALLAH, and then my Parents and Siblings.

ACKNOWLEDGEMENT

In the name of Allah, the Most Beneficent and the Most Merciful, all praises and adorations are due to Him, the Creator of heaven and earth, the Lord of the worlds. Despite the numerous efforts put into this research work, it would not have been possible without the help of Almighty God, the fountain of all wisdom, knowledge and understanding.

I wish to express my deepest gratitude to my supervisor and teacher Dr. S.M. Sani, for his tireless efforts, valuable guidance, advice and constant supervision towards the success of this work. The completion of this work could not have been possible without your constant participation and assistance. My thanks also goes to my co-supervisor Dr. A.M.S. Tekanyi for his encouragement, advice and support. Words are not enough to express my gratitude to you both. May Almighty ALLAH never leave you alone to your affairs.

My sincere and unending appreciation also goes to Etisalat Nigeria for the life time opportunity they gave me through their initiative and support for the masters in telecommunication engineering program, Etisalat Telecommunication Engineering Program (ETEP).

I acknowledge with thanks all the lecturers of Electrical and Computer Engineering, Ahmadu Bello University, namely: Prof. B. G. Bajoga, Prof. M.B. Mu'azu, Prof. B. Jimoh, Dr. Y. Jibril, Dr. A. D. Usman, Dr. S. Garba, Dr. T.H Sikiru, Dr. K.A. Abu-Bilal, Engr.F. Sadiku, Engr. M. J. Mu'azu, Engr. A. I. Abdullahi, Engr. E. A. Olarinoye, Engr. Bashir Sadiq, Engr. Salawudeen A. Tijjani, Engr. Olaniyan Abdulrahman and most especially, those whose names could not be mentioned. My deepest appreciation also goes to Engr. Ovie and Oyibo Prosper for all their support.

I am also thankful to my special friends, Magaji Suleiman, Ajayi Ore-Ofe, Braimoh Jinadu, Ocholi H., Ibrahim Abdulwahab, Aboo Aasiyah, Hajia Mairo, Abdulrasheed, Mr. Aliyu Ahmed,

Ibrahim Ladan, Aminu Abba, Atuman G. Joel, Alhassan, and Engr. Suleiman Hussein, Daddy Jessi, Malachi Egbugha. Oga Abubakar, Muktar Abubakar. Their continuous support and contributions toward the success of this work would never be forgotten, may God reward them and strengthen our friendship.

Above all, I am overly indebted to my dear parents Mr & Mrs A. Ajadi, your endless love, prayers, support, kindness and understanding personality will always be appreciated. Thank you very much. My gratitude will be incomplete until I acknowledge the efforts and supports of my siblings, Ummu Abdulsalaam, Ummu Aa'isha, Ummu Fareedah, Aboo Tau'amayn, Yoosuf and their spouses. May Allah continue to strength the bond of blood and Islam between us and admit us all into the highest place in His paradise, Amen.

Wasiu Olayinka AJADI
March, 2017.

ABSTRACT

Cognitive radio (CR) has been suggested as the solution to spectrum scarcity due to the fixed allocation employed worldwide by regulatory bodies. A secondary user can opportunistically access the licensed frequency bands without causing harmful interference to the licensed user. In order to avoid interference to a primary user signal, the CR has to be aware about the spectrum usage in the geographic area in which it wants to operate. The process of spectrum sensing is a fundamental task for obtaining this awareness and the result of this process determines the successful operation of cognitive radio. Energy detection is one of the methods of spectrum sensing with the lowest computational complexity but with low performance at low signal to noise ratio. Exploring energy detection has led to the application of many techniques one of which is the use of time-frequency analysis. This method employs distribution techniques for analyzing the energy spectral density of an observed signal with a view to setting a sensing threshold. However, the distribution techniques that were used in literature suffered from the problem of cross-terms which affect the analysis of the resulting distribution thereby leading to poor sensing performance at low signal-to-noise ratio. Smoothed pseudo Wigner-Ville distribution (SPWVD) of the time-frequency analysis has been employed in this work to reduce the effect of cross-terms and a better sensing threshold was gotten validated through comparison with the existing work which employed pseudo Wigner-Ville Distribution (PWVD) with an average reduction of 2.7% and 3% for additive white Gaussian noise (AWGN) channel, 4.1% and 4.7% for Rician channel, 6.4% and 8% for Rayleigh channel in the probabilities of missed detection and false alarm respectively. These results showed that significant reduction was achieved using SPWVD to set threshold. This work was carried out using the MATLAB R2013b time-frequency tool box.

TABLE OF CONTENTS

TITLE PAGE	i
DECLARATION	II
CERTIFICATION	III
DEDICATION	iv
ACKNOWLEDGEMENT	v
ABSTRACT	VII
LIST OF FIGURES	xi
LIST OF TABLES	xii
LIST OF ABBREVIATION	xiii
CHAPTER ONE: INTRODUCTION	
1.1 Background of Study	1
1.2 Problem Statement	4
1.3 Aim and Objectives	4
1.4 Methodology	5
1.5 Significance of the Research	5
1.6 Organization of the Dissertation	6
CHAPTER TWO: LITERATURE REVIEW	
2.1 INTRODUCTION	7
2.2 Review of Fundamental Concepts	7
2.2.1 Cognitive Radio Concepts	7
2.2.2 Secondary User Spectrum Measurement	9
2.2.3 Spectrum Sensing	12
2.2.4 Spectrum Sensing Techniques	12
2.2.5 Time-Frequency Analysis (TFA) for Energy Detection	15
2.2.6 Cross-Terms (Interference Component)	15

2.2.7	Kernels for Suppressing Cross-Terms	16
2.2.8	Analytic Associate	17
2.2.9	Ambiguity Domain	17
2.2.10	Time-Frequency Distribution Techniques	17
2.2.10.1	<i>Wigner-Ville Distribution</i>	18
2.2.10.1	<i>Pseudo Wigner-Ville Distribution</i>	19
2.2.10.1	<i>Choi Williams Distribution</i>	19
2.2.10.1	<i>Cove Shaped Distribution</i>	20
2.2.10.1	<i>Smoothed Pseudo Wigner-Ville Distribution</i>	21
2.2.11	Wireless Channel Model	21
2.2.12	Comparison Metrics	25
2.3	REVIEW OF SIMILAR WORKS	25
CHAPTER THREE: MATERIALS AND METHODS		
3.1	Introduction	34
3.2	System Model	34
3.3	Signal Simulation Process	35
3.3.1	AWGN Channel	37
3.3.2	Rayleigh Channel	37
3.3.3	Rician Channel	37
3.4	Hilbert Transforming the Simulated Signal	38
3.5	Smoothing and Calculating ESD using SPWDV	41
3.6	Threshold Determination	43
3.7	GLRT on the Set Threshold	43
3.8	Performance Metrics	44
3.8.1	Probability of False Alarm	44

3.8.2	Probability of Missed Detection	45
3.8.3	Signal to Noise Ratio	46
3.8.4	Relationship between PFA, PMD and SNR	46
CHAPTER FOUR: RESULT AND DISCUSSION		
4.1	Introduction	48
4.2	Results of Comparisons	48
CHAPTER FIVE: CONCLUSION AND RECOMMENDATION		
5.1	Summary	57
5.2	Conclusion	57
5.3	Significant Contribution	58
5.4	Recommendations	58
	REFERENCES	59

LIST OF APPENDICES

APPENDIX A		
OFDM SIMULATIONmFILE CODE		63
APPENDIX B		
RAYLEIGH CHANNELmFILE CODE		67
APPENDIX C		
RICIAN CHANNELmFILE CODE		68
APPENDIX D		
OFDM PARAMETERSmFILECODE		69
APPENDIX E		
OFDM BASE CONVERSIONmFILE CODE		71
APPENDIX F		
OFDM MODULATIONmFILE CODE		72
APPENDIX G		
	SPWVDmFILE CODE	74
APPENDIX H		
	PWVDmFILE CODE	76
APPENDIX I		
CONDITIONAL PROBABILITYmFILE CODE		78

LIST OF FIGURES

Figure 2.1: Cognitive Radio Cycle	8
Figure 2.2: Interweave Mode of Operation	9
Figure 2.2: Underlay Mode of Operation	9
Figure 3.1: Spectrum Sensing Scenario	35
Figure 4.1: Plot of PMD against SNR for AWGN Channel	49
Figure 4.2: Plot of PFA against SNR for AWGN Channel	50
Figure 4.3: Plot of PMD against SNR for Rician Channel	51
Figure 4.4: Plot of PFA against SNR for Rician Channel	52
Figure 4.5: Plot of PMD against SNR for Rayleigh Channel	54
Figure 4.6: Plot of PFA against SNR for Rayleigh Channel	55

LIST OF TABLES

Table 3.1: OFDM Simulation Parameters	38
Table 4.1: Data for SPWVD and PWVD with PMD for AWGN Channel	49
Table 4.2: Data for SPWVD and PWVD with PFA for AWGN Channel	50
Table 4.3: Data for SPWVD and PWVD with PMD for Rician Channel	51
Table 4.4: Data for SPWVD and PWVD with PFA for Rician Channel	52
Table 4.5: Data for SPWVD and PWVD with PMD for Rayleigh Channel	53
Table 4.6: Data for SPWVD and PWVD with PFA for Rayleigh Channel	55

LIST OF ABBREVIATIONS

Acronyms	Definition
CR	Cognitive Radio
PU	Primary User
SU	Secondary User
ED	Energy Detection
TFA	Time-Frequency Analysis
TFD	Time-Frequency Distribution
WVD	Wigner-Ville Distribution
PWVD	Pseudo Wigner-Ville Distribution
CWD	Choi Williams Distribution
CSD	Cone Shaped Distribution
SPWVD	Smoothed Pseudo Wigner-Ville Distribution
GLRT	Generalized Likelihood Ratio Test
AWGN	Additive White Gaussian Noise
SNR	Signal to Noise Ratio
PMD	Probability of Missed Detection
PFA	Probability of False Alarm

CHAPTER ONE

INTRODUCTION

1.1 Background of Study

Electromagnetic spectrum is one of the most important resources required for radio communications. Spectrum utilization is regulated throughout the world so that essential services can be provided and also protected from harmful interference. Spectrum governance across the world traditionally tended toward static long-term exclusive use of spectrum, assigning license to a specific operator on a certain frequency band, thereby, giving them the exclusive right to operate on the licensed band (Biglieri *et al.*, 2012). This static spectrum allocation strategy has led to many successful applications like broadcasting and mobile communication and it has also led to almost the entire prime available spectrum being assigned for various applications (Biglieri *et al.*, 2012). It may thus seem that there is little or no spectrum available for emerging wireless products and services.

There had been several studies and reports over the years that showed that the static allocated spectrum was in fact vastly underutilized. A report presenting statistics regarding spectrum utilization showed that even during the high demand period of a political convention such as the one held in 2004 in New York City, only about 13% of the spectrum opportunities were utilized (McHenry & McCloskey, 2004). Further, measurement on radio frequency bands from 30 MHz to 910 MHz was done in Mexico City of San Luis Potosi and showed 11.83% (Aguilar-Gonzalez *et al.*, 2013), Kwara State of Nigeria at 48.5 MHz to 880 MHz showed 12.02% usage in the urban areas (Babalola *et al.*, 2015), and also at 2.4GHz to 2.7GHz showed 22.56% usage in the urban areas (Ayeni *et al.*, 2016), thus, all showing that spectrum was in fact underutilized. These findings also suggest that devices using advanced radio and signal processing technology should

be able to exploit underutilized spectrum. Much of the early motivation for cognitive radio technology was indeed to accomplish such opportunistic spectrum use and to also alleviate the artificial scarcity of prime spectrum. This technology could revolutionize the way spectrum is allocated worldwide (Biglieri *et al.*, 2012).

Cognitive radio (CR) is the key enabling technology for the implementation of dynamic spectrum access (DSA) which has been suggested as one of the most potent remedial measures for the fixed spectrum allocation which has led to spectrum scarcity (Weiss *et al.*, 2012). A CR is an evolved software defined radio (SDR) that has the ability to analyze its surrounding radio environment and decide how best to re-configure itself to suit operations without causing harmful interference to the licensed user (Javed & Mahmood, 2010). The CR has the ability to identify any opportunities that exist in the spectrum band of interest and utilize them without causing any interference to the primary users (PUs). These opportunities exist in the form of spectrum holes or white spaces. A spectrum hole is the part of the spectrum that is devoid of the primary licensed user.

The major functions of CR are: spectrum sensing which is the process of identifying the presence of licensed users and unused frequency bands, that is, white spaces in those licensed bands; spectrum management which is identifying how long the secondary users can use those white spaces; spectrum sharing which is the decision process of how to share the white spaces (spectrum hole) fairly among the secondary users; and spectrum mobility which is maintaining seamless communication during the transition from one spectrum band to another when a primary user is sensed on the current band of transmission (Mounika *et al.*, 2013).

In order to avoid interference to a primary user signal, the CR terminal has to be aware about the spectrum usage in the geographic area in which it wants to operate. Spectrum sensing is a

fundamental task for obtaining this awareness(Angrisani *et al.*, 2014). The challenging task is carrying out reliable spectrum sensing at low signal-to-noise ratio (SNR) as the successful operation of CR depends on the result of spectrum sensing. This means that a secondary user needs to reliably detect a primary user that is transmitting at very low power or that is located far from the detection point. The selection of the most appropriate spectrum sensing technique should take into account the trade-off between the performance and the computational burden(Angrisani *et al.*, 2014).

Spectrum sensing can be done for detecting spectrum holes opportunity in which the cognitive radio can only transmit when the primary user is not transmitting or interference temperature detection in which case the cognitive radio is allowed to coexist with the primary user but transmitting at very low power in order not to cause interference to the primary user (Mounika *et al.*, 2013).

Various spectrum sensing techniques have been researched for detecting spectrum holes opportunity among which are: energy detection, cyclostationary feature detection and matched filtering (Vaidehi *et al.*, 2015). All these techniques perform well at high signal to noise ratio. Energy detection has the lowest computational burden but also has low detection performance compared to others, especially at very low signal to noise ratios (Arthy & Periyasamy, 2015). Its low computational complexity is what attracts attention from researchers and that it does not require information of the primary user transmission which is a limitation in other detection techniques.

Earlier works on energy detection presented different ways of achieving a good spectrum sensing performance under varying signal to noise ratios and users, one of which is the method of time-frequency analysis using Wigner-Ville distribution. This work will focus on improving the

sensing threshold of energy detection using a different distribution technique of time-frequency analysis. This technique will improve on the weakness of the earlier distributions techniques that have been employed.

1.2 Problem Statement

The successful operation of cognitive radios depends largely on the results of spectrum sensing. Energy detection being the simplest to implement in terms of computational complexity has attracted a great deal of attention from researchers in order to improve on it, as its performance is weak when the SNR is low. Researches had proposed ways of performing energy detection and the use of time-frequency analysis show a great potential. However, the distribution techniques used so far suffers from cross-terms which affects the readability of the resulting distribution, leading to no improvement on the sensing threshold. Therefore, there is the need to employ a different distribution technique that can improve on the weakness of the techniques present in literature so as to improve on the sensing threshold, especially at low signal to noise ratio.

1.3 Aim and Objectives

The aim of this work is to determine an improved spectrum sensing threshold for energy detection through the use of time-frequency analysis by employing smoothed pseudo Wigner-Ville distribution to analyze the energy spectral content of the primary user signal. The research work had the following objectives:

1. To simulate signals of an orthogonal frequency division multiple access (OFDMA) user with varying signal-to-noise ratios.

2. To apply the smoothed pseudo Wigner-Ville distribution technique on the generated signals to determine the energy spectral content and determining a better sensing threshold.
3. To compare the result obtained with the work of Monfared et al., (2013) in order to establish the validity and improvement made of the technique used in this work.

1.4 Methodology

The following steps will be taken to achieve the set objectives:

1. Simulation of an OFDMA signal in MATLAB R2013b environment to get a primary user signal.
2. Performing the Hilbert transform of the simulated signal to get the analytic associate of the signal.
3. Calculating the energy density of the signal in terms of the time and frequency using the smoothed pseudo Wigner-Ville distribution technique in the MATLAB R2013b time frequency toolbox.
4. Steps 1, 2 and 3 were repeated for a hundred simulations and the mean energy density was taken in order to set a threshold.
5. Taking generalized likelihood ratio test to detect the presence or absence of a primary user based on the set threshold.
6. Comparing the performance of this method with the work of Monfared et al., (2013) to establish the validity as well as show improvement achieved.

1.5 Significance of the Research

The Wireless Regional Area Network (WRAN) under the IEEE 802.22 working group specify that for successful cognitive radio operation that opportunistically access a licensed spectrum as

the secondary user must be able to detect the presence of spectrum holes (absence of the primary user) with high level of precision that ensures minimum interference on the primary user. Earlier works on the use of time-frequency analysis for energy detection of the primary user transmitter has demonstrated a great potential of meeting the requirement of the standardization body hence, this research work was embarked on to further improve the performance of the technique by adopting smoothed pseudo Wigner-Ville distribution in order to better the limitation of the earlier research works.

1.6 Organization of the Dissertation

The organization of this dissertation report is as follows: Chapter one presents the general background of the study. Chapter two discussed the review of fundamental concepts pertinent to the research work and detailed review of similar works was presented. In chapter three, the methods and materials adopted in this research are presented and explained in details. Chapter four presents the results and discussions and lastly in chapter five, conclusions and recommendations were discussed. Finally, all the references quoted in this dissertation report and appendices were provided.

CHAPTER TWO

LITERATURE REVIEW

2.1 Introduction

In this section, the literature review comprising the review of fundamental concepts and the review of similar works are presented. The theoretical framework guiding researches in this area in addition to contributions by other researchers are discussed in the following sections.

2.2 Review of Fundamental Concepts

The cognitive radio concepts and spectrum sensing techniques are discussed with the fundamentals which are background to this research work. The approach and technique that contributed to the achievement of our aim of this work were identified through this discussion.

2.2.1 Cognitive Radio Concepts

Cognitive Radio (CR) is software defined radio that has the ability to sense its operational environment and can dynamically and autonomously adjust its radio operating parameters to modify its operation, by maximizing throughput and mitigating interference, as well as facilitating interoperability and access spectrum holes as a secondary user (Kolodzy & Avoidance, 2002). The cognitive-radio device functions in the following closed cycle stages of Observe-Decide- Act-Learn cognitive cycle as in Figure 2.1. These are based on the following (Christodoulou & Jayaweera, 2011):

1. Observing the primary user transmission activity in the channel,
2. Deciding which part of the spectrum is free for transmission,
3. Acting appropriately to achieve the required mode of transmission, and
4. Learning from previous primary user activity in the channel.

This cycle allows the cognitive-radio device to decide and reconfigure its transmission parameters (Christodoulou & Jayaweera, 2011).



Figure 2.1: Cognitive Radio Cycle (Christodoulou & Jayaweera, 2011).

A cognitive-radio device operates in either the “interweave” or the “underlay” mode for better spectrum efficiency (Tawk *et al.*, 2014). In both types of operation, the unoccupied parts of the spectrum are referred to as white spaces or spectrum holes.

Interweave mode of operation, as in Figure 2.2, requires that the cognitive radio search for white spaces and decide which white space to allocate for secondary users under specific rules. The secondary users can transmit in this case without any power constraint. The underlay mode, as in Figure 2.3, also requires searching for white spaces even though, the secondary user can co-exist with the primary user by transmitting below the allowed interference level of primary users. For

this case, there is a constraint on the transmit power of the secondary users, since both primary and secondary users can occupy the same frequency bands at a time (Tawk *et al.*, 2014).

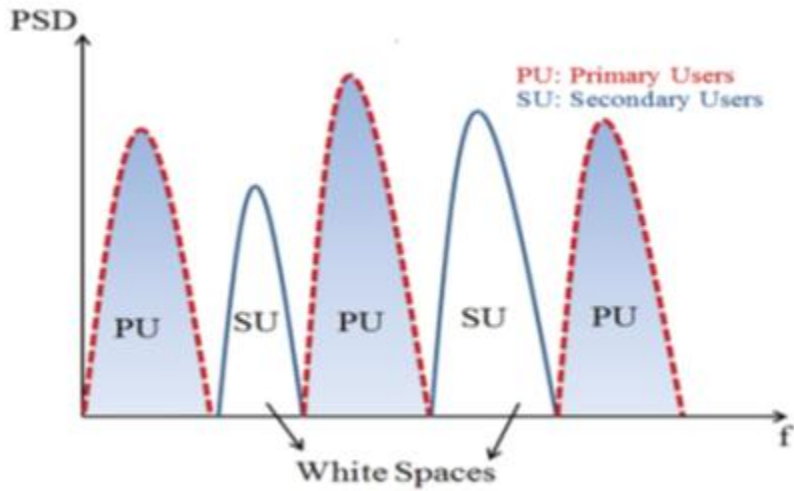


Figure 2.2: Interweave Mode of Operation (Tawk *et al.*, 2014).

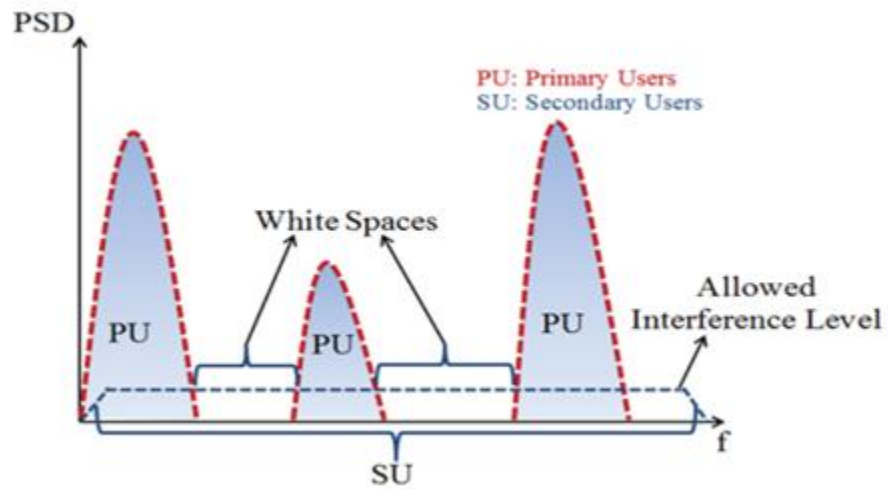


Figure 2.3: Underlay Mode of Operation (Tawk *et al.*, 2014).

2.2.2 Secondary User Spectrum Measurements

The secondary user is responsible for ensuring that it creates no undue interference to primary users of the relevant spectrum. According to the IEEE 802.22 WRAN working group, the secondary user network is made up of the base station, BS, and a number of user equipment known as customer premises equipment, CPE (IEEE 802.22.2-2012, 2012).

In order to effectively use the spectrum holes opportunity, spectrum sensing is distributed across the network of users. Accordingly, the 802.22 spectrum sensing is undertaken within the Customer Premises Equipment, CPEs. The CPEs scan the various channels that are open for their use and send back information about signals and strengths on the channels to the base station equipment. It is BS which makes the decision about which channels are occupied and whether they can be used for the secondary user transmissions (IEEE 802.22.a-2014, 2014). The BS uses the spectrum sensing results as well as geo-location information and other information provided by an entity known as the network manager to make the decision of whether transmission can start or not. The base station instructs the CPEs to perform periodic measurements in one of two formats (IEEE 802.22.a-2014, 2014);

1. **In band spectrum sensing:** The in-band spectrum sensing applies to the channels that are being currently used by the BS to communicate with the CPEs. This type of sensing requires that the BS quieten the transmissions on the channel (seizes transmission for a certain period in order to carry out the spectrum measurement). When assessing the presence of primary user signals on the channel, the CPE is required to look for very low level, the levels required and the accuracy being controlled by the BS (Ian, 2016). In order to gain the best overall measurement, the BS may instruct different CPEs to make different measurements (this is a case of cooperative spectrum sensing scenario which still depends on spectrum sensing information from each secondary user in the network).

The choice of how this is done is made by the BS and it's calculated by the algorithms it contains. By instructing different CPEs to make different measurements and over different lengths of time, the BS make up an occupancy map for the overall cell (Ian, 2016).

2. **Out of band spectrum sensing:** The out of band spectrum sensing refers to measurements over the channels that are not currently being used by the BS to communicate with the CPEs. These measurements are taken in order to locate possible alternative channels, when the primary is perceived to have resume transmission on the present channel (Ian, 2016). It also ensures that there is a sufficient guard band between the channels in use by the BS and any primary user that may be using adjacent channels.

The in-band spectrum sensing is carried out on a regular basis. The quiet periods for sensing are built into the transmission frame timings. There are two types of sensing that are defined:

1. **Fast sensing:** This form of spectrum sensing is taken quickly. This sensing typically uses a simple energy detection algorithm and is completed within very small amount of time (1ms is required according to the standardization body). The results of the fast sensing are returned to the BS which then analyses them and determines whether a fine sensing measurement is required (Ian, 2016). This type of spectrum sensing is what this research work set to accomplish.
2. **Fine sensing:** The fine sensing is undertaken when there is the need for a more accurate measurement. During the fast sensing a more detailed examination is made of the particular channels. This form of spectrum sensing takes longer time than the fast sensing, typically around 25ms is required according to the standardization body. The fine sensing also checks for possible adjacent 802.22 networks that may cause

interference to one another, and the adjacent networks may sense each other (Ian, 2016). To overcome the possibility of confusion caused by adjacent networks detecting each other algorithms are built into the system to synchronize overlapping cells. This also includes the synchronization of the quiet periods when the spectrum sensing occurs.

2.2.3 Spectrum Sensing

The process of observing primary users’ activity in order to detect white spaces or spectrum holes is known as spectrum sensing (Tawk *et al.*, 2014). White space is the part of a spectrum devoid of primary user activity, dependent on time, space and frequency. There are various ways to sense a spectrum for white space and these techniques can be categorized based on whether the technique requires information of the primary user such as pulse shape, data rate, bandwidth, carrier frequency, modulation technique, and so on.

2.2.4 Spectrum Sensing Techniques

The major spectrum sensing techniques are as follows:

1. **Energy Detection:** This is the most widely researched, owing to its simplicity and non-requirement of primary user transmission information. It estimates the presence of primary user by comparing the energy received with a set threshold derived from the statistics of the noise (Subhedar & Birajdar, 2011). The threshold value can be fixed or variable based on the channel conditions. Signal detection can be reduced to a simple identification problem, formalized as a hypothesis test:

$$z(n) = x(n) \dots\dots\dots H_0 \tag{2.1}$$

$$z(n) = x(n) + h(n) \dots\dots\dots H_1 \tag{2.2}$$

where:

$z(n)$ is the sample to be analyzed at each instant “n”

$x(n)$ is the noise of variance σ^2 .

$h(n)$ is the actual signal transmitted

\mathbf{H}_0 denotes the absence of primary user transmission

\mathbf{H}_1 denotes the presence of the primary user transmission.

Assuming $z(n)$ is a sequence of received samples $n \in \{1, 2, \dots, N\}$ at the signal detector, then a decision rule can be stated as,

$$\mathbf{H}_0 \text{ if } E < T \tag{2.3}$$

$$\mathbf{H}_1 \text{ if } E > T \tag{2.4}$$

where:

$E = \int |z(n)|^2$ the estimated energy of the received signal

T is the set threshold, chosen depending on the noise variance σ^2 .

The energy detector is easy to implement and requires no prior information about the primary user (PU) signal. However, the uncertainty of noise power imposes fundamental limitations on the performance of the energy detector (Jouini, 2011) and (Tandra & Sahai, 2008a). Below an SNR threshold, a reliable detection cannot be achieved by increasing the sensing duration. This SNR threshold for the detector is called SNR wall (Tandra & Sahai, 2008b).

2. **Cyclostationary Feature Detection:** Cyclostationarity-based detection analyzes the cyclic autocorrelation function of the received signal, which is periodic for data signals, but aperiodic for noise and generally, for wide-sense stationary signals (Gardner, 1991). The periodicity inherent in the primary signals are related to carrier frequency, symbol, hop rate, etc., and they can often be assumed as known. However, synchronization errors

may affect the detection procedure and also it is computationally complex (Biglieri *et al.*, 2012).

3. **Matched Filtering:** Matched filter operation is equivalent to correlation in which the unknown signal is convolved with the filter whose impulse response is the mirror and time shifted version of a reference signal. The operation of matched filter detection is expressed as:

$$z(n) = \sum_{n=-\infty}^{\infty} h(y-n)x(n) \quad (2.5)$$

where x is the unknown signal and is convolved with the h , the impulse response of matched filter, that is matched to the reference signal for maximizing the SNR (Subhedar & Birajdar, 2011).

It requires perfect knowledge of the primary signal such as bandwidth, modulation type, etc. The sensing receiver should also be able to synchronize to the received PU signal, which is an unreasonable assumption in typical spectrum sensing scenarios. The sensing receiver should also implement most of the specific waveform processing functions of the corresponding PU receiver, which would lead to high complexity. For these reasons, matched filter based detection is not considered as a relevant choice in cognitive radios (Dikmese, 2015).

There are other spectrum sensing techniques such as radio mode identification, waveform based and others but they also require prior knowledge of the primary user signals which makes them computationally complex even though they might achieve better sensing accuracy than the energy detection scheme. The energy detection's simplicity and non-requirement of primary user information makes it the most widely researched. Time-

frequency analysis distribution techniques have been researched in order to improve on its detection accuracy.

2.2.5 Time-Frequency Analysis (TFA) for Energy Detection

Time-frequency analysis is used to analyze and process time varying signal in order to spread the energy of the signal component in the time and frequency domains simultaneously. The result of the processing may then exploit the features of the signal in the two planes rather than one (Boashash, 2015).

There are two classical ways of representing a signal: the time-domain representation $s(t)$ and the frequency-domain representation $S(f)$. In both forms, the variables t and f are treated as mutually exclusive. To obtain a representation in terms of one variable, the other variable is "integrated out". Consequently, each classical representation of the signal is non-localized with respect to the other excluded variable, that is, the frequency representation is averaged over the values of the time representation at all times and the time representation is averaged over the values of the frequency representation at all frequencies (Boashash, 2015).

There are several time-frequency distribution techniques that can be explored for the purpose of analysis. One of the pioneer techniques is the Wigner-Ville distribution but it suffers from cross-term effects which has impact on the resolution of the resulting analyzed signal (Boashash, 2015). Other distribution techniques have been developed with different signal kernels and that offer different compromise between suppression of cross-terms and blurring in the resolution of the resulting signal distribution.

2.2.6 Cross-Terms (InterferenceComponents)

Cross-terms are artifacts that appear in the Wigner-Ville distribution (WVD) representation between auto-terms, which correspond to physically existing signal components. These cross-terms falsely indicate the existence of signal components between auto-terms. Localizing signals in time and frequency domains simultaneously requires that the distribution techniques should be a bilinear function. This bilinear function follows a quadratic superposition principles (Boashash, 2015) defined as:

$$W_{x+y}(t, v) = W_x(t, v) + W_y(t, v) + 2\mathcal{R}\{W_{x,y}(t, v)\} \quad (2.6)$$

But,

$$W_{x,y}(t, v) = \int_{-\infty}^{+\infty} x\left(t + \frac{\tau}{2}\right) y * \left(t - \frac{\tau}{2}\right) e^{-j2\pi v\tau} d\tau \quad (2.7)$$

$W_{x,y}(t, v)$ is the cross-term present in the resulting cross product of signal x and y.

where:

$W(t, v)$ denote the Wigner-Ville distribution of signal 'x'

't' is the time

' τ ' is a delay in time or time shift

'v' is a delay in frequency or Doppler shift

These cross-terms overlap with the auto-terms (signal terms), thereby affecting the readability of the resulting distribution.

2.2.7 Kernels for Suppressing Cross-Terms

Cross-terms can make the WVD difficult to interpret, especially if the components are numerous or close to each other, and more so in the presence of noise. Cross-terms between signal components and noise exaggerate the effects of noise and cause rapid degradation of performance as the SNR decreases. The desire to suppress them has led to the development of smoothing functions or kernel which minimizes the effect of cross-terms along the time and frequency domains. The kernel can be coupled where the smoothing is done along frequency domain or separable where the smoothing is done along both time and frequency domains independent of each other.

2.2.8 Analytic Associate

A real signal usually exhibit Hermitian symmetry between positive and negative frequencies which allow the deduction of the negative from the positive frequency. The negative frequency can then be removed from the positive without losing information and this has the advantage of halving the required bandwidth and avoids the interference generated between the positive and negative frequencies (Boashash, 2015). This can be achieved by performing the Hilbert transform on the real signal and the resulting signal is what is known as the analytic associate or signal. All time-frequency distribution techniques are applied on the analytic associate of the real signal.

2.2.9 Ambiguity Domain

This is the frequency lag or Doppler lag domain where time-shift and frequency shift in the signal are almost equivalent. It is at this point where most of the other distribution techniques tried to reduce the effect of cross-terms. Most of them tend to smoothen the cross-term problem along the frequency domain except for the smoothed pseudo Wigner-Ville distribution owing to its design of separable kernel functions along the time and frequency domains distinctively.

2.2.10 Time-Frequency Distribution Techniques

The following are some of the time-frequency distribution techniques

1. Wigner-Ville Distribution
2. Pseudo Wigner-Ville Distribution
3. Choi Williams Distribution
4. Cone Shaped Distribution
5. Smoothed Pseudo Wigner-Ville Distribution

2.2.10.1 Wigner-Ville distribution:

The Wigner-Ville distribution (WVD) is a good choice when extracting features from a signal that contains only a single component. The disadvantage of the WVD is cross-term interference. Cross-terms are artifacts that appear in the WVD representation between auto-terms, which correspond to physically existing signal components. These cross-terms falsely indicate the existence of signal components between auto-terms(Boashash, 2015).The WVD on the whole gives better temporal and frequency resolution at the expense of many artifacts and the introduction of negative values, which would correspond to negative energy, that is not physically possible to represents a significant defect in this method(Boashash, 2015). These are known issues with the WVD, and there are ways to compensate them, which has led researches into developing reduced interference distribution techniques. They all derive from the WVD but with different smoothing functions known as kernel. WVD technique is given by (Boashash, 2015) as follows;

$$W(t, f) = \frac{1}{2\pi} \int s^*(t - \frac{1}{2}\tau) s(t + \frac{1}{2}\tau) e^{-j\tau 2\pi f t} d\tau \quad (2.8)$$

where:

' t ' is the time of occurrence of signal ' s '

' τ ' is a delay in time or time shift

' f ' is the frequency

2.2.10.2 *Pseudo Wigner-Ville distribution:*

The pseudo Wigner-Ville distribution (PWVD) is essentially the same as the original WVD. The PWVD adds a window kernel function to smoothen out the cross terms generated in the original WVD, but the effect of cross terms is only slightly reduced. The distribution is given as (Boashash, 2015):

$$PW(t, f) = \frac{1}{2\pi} \int h(\tau) s^*(t - \frac{1}{2}\tau) s(t + \frac{1}{2}\tau) e^{-j\tau 2\pi f t} d\tau \quad (2.9)$$

where:

' t ' is the time of occurrence of signal ' s '

' τ ' is a delay in time or time shift

' f ' is the frequency

$h(\tau)$ is the smoothing function along the frequency domain

2.2.10.3 *Choi-Williams distribution:*

The Choi-Williams distribution (CWD) uses an exponential kernel function. The exponential kernel function has the same dimensions as the ambiguity function. The CWD reduces the cross-terms generated by two auto-terms with different time centers and frequency centers (Boashash,

2015). The CWD possesses useful properties of the WVD, such as accurate marginal time integration, marginal frequency integration, mean instantaneous frequency, and group delay. The CWD has a coarser time-frequency resolution than the WVD, because the CWD blurs the auto-terms when the CWD reduces the cross-terms (National Instruments, 2016). The CWD does not suppress the cross-terms that have two auto-terms with the same time center or frequency center generated. The exponential kernel function includes an alpha parameter to balance the cross-term suppression and the blurriness of auto-terms. The larger the value of the alpha parameter, the better the cross-term suppression and the more blurry auto-terms become (National Instruments, 2016). The technique is given as (National Instruments, 2016):

$$W_{cw}(t, f) = \left(\int \sqrt{\frac{\sigma}{4\pi\tau^2}} e^{-\sigma-t^2/4\tau^2} \right) \times \int s\left(t + \frac{\tau}{2}\right) s^*\left(t - \frac{\tau}{2}\right) e^{-j2\pi f\tau} d\mu d\tau \quad (2.10)$$

where:

‘ t ’ is the time of occurrence of signal ‘ s ’

‘ τ ’ is a delay in time or time shift

‘ f ’ is the frequency

‘ σ ’ is a smoothing parameter in the frequency domain, and the first integral terms are the smoothing function.

2.2.10.4 *Cone-shaped distribution:*

The cone-shaped distribution (CSD) kernel function suppresses the cross-terms away from the frequency axis and the origin of the ambiguity function plane. The CSD suppresses the cross-terms that have two auto-terms with different time centers and frequency centers generate (Boashash, 2015). Additionally, the CSD suppresses the cross-terms that the two auto-terms with the same frequency center generate. The CSD cannot reduce cross-terms that the two

auto-terms with the same time center generated(National Instruments, 2016). The technique is given in the below equation (National Instruments, 2016):

$$C_x(t, f) = \iint \left(\frac{\sin(\pi\mu\tau)}{\pi\mu\tau} e^{-2\pi\alpha\tau^2} \right) d\mu d\tau \times s\left(t + \frac{\tau}{2}\right) s^*\left(t - \frac{\tau}{2}\right) e^{-j2\pi\mu t} dt \quad (2.11)$$

where:

‘ t ’ is the time of occurrence of signal ‘ s ’

‘ τ ’ is a delay in time or time shift

‘ f ’ is the frequency

‘ μ ’ is the smoothing parameter in the time domain

2.2.10.5 Smoothed pseudo Wigner-Ville distribution

This distribution is as given in the equation below (Auger *et al.*, 2005):

$$SPWVD_x(t, v) = \int_{-\infty}^{\infty} h(\tau) \int_{-\infty}^{\infty} g(v - t) s\left(t + \frac{\tau}{2}\right) s^*\left(t - \frac{\tau}{2}\right) ds e^{-j2\pi v t} d\tau \quad (2.12)$$

where:

‘ t ’ is the time of occurrence of signal ‘ s ’

‘ τ ’ is a delay in time or time shift

‘ v ’ is the frequency shift or Doppler shift

$h(t)$ and $g(s - t)$ are the separate smoothing functions along the time and frequency domains respectively.

The separable smoothing functions give a degree of freedom to the designer in order to have a compromise between joint time-frequency resolution and cross-terms suppression depending on the area of application.

2.2.11 Wireless Channel Models

The path between transmitting and receiving antenna is generally termed as wireless channels and these channels impact on the characteristics of the transmitted signal as it travels depending on the condition of the terrain. The signal characteristics are due to several phenomena (Viswanathan, 2013): (i) existence of line of sight path between the antennas, (ii) reflection, refraction and diffraction of the signal due to the objects in between the antennas, (iii) The relative motion between the transmitter and receiver and the objects in between them, (iv) The signal attenuation as it travels through the medium, (v) Noise in the channel. The received signal can be obtained from the transmitter signal if the channel in between the antennas can be accurately modeled. It is quite difficult to model the real world environment. Scientists and engineers have studied various environments and provided ways to model the various medium that approximate the real world environments. Three wireless channels were considered in this work namely: Additive White Gaussian Noise (AWGN), Rician and Rayleigh Channels.

1. **Additive White Gaussian Noise (AWGN) Channel:** Additive White Gaussian Noise (AWGN) is the statistically random radio noise characterized by a wide frequency range with regards to signal in communications channel. It is the accepted model for thermal noise in communication channels, with the assumptions that (Viswanathan, 2013): (i) the noise is additive, that is, the received signal equals the transmit signal plus some noise, where the noise is statistically independent of the signal, (ii) the noise is white, that is, the power spectral density is flat, so the autocorrelation of the noise in time domain is zero for any non-zero time offset, (iii) the noise samples have a Gaussian distribution.
2. **Multipath Channel:** A multipath fading channel can be modeled as an FIR (Finite Impulse Response)-filter with the following impulse response (Viswanathan, 2013):

$$\mathbf{h}(\boldsymbol{\tau}, \mathbf{t}) = \mathbf{h}_0(\mathbf{t})\delta(\boldsymbol{\tau} - \boldsymbol{\tau}_0(\mathbf{t})) + \mathbf{h}_1(\mathbf{t})\delta(\boldsymbol{\tau} - \boldsymbol{\tau}_1(\mathbf{t})) + \cdots + \mathbf{h}_{n-1}(\mathbf{t})\delta(\boldsymbol{\tau} - \boldsymbol{\tau}_{N-1}(\mathbf{t})) \quad (2.14)$$

Where $\mathbf{h}(\boldsymbol{\tau}, \mathbf{t})$ is the time varying impulse response of the multipath fading channel having N multi-paths and $\mathbf{h}_i(\mathbf{t})$ and $\boldsymbol{\tau}_i(\mathbf{t})$ denote the time varying complex gain and excess delay of the i-th path.

Multipath fading channel can be modeled such that the impulse response may follow distributions like Rayleigh distribution (no Line of Sight (LOS) ray between transmitter and receiver) or as Rician distribution (a dominant LOS path exist between transmitter and receiver), Nagami distribution, Weibull distribution etc. (Viswanathan, 2013). Rayleigh and Rician multipath channels were used in this work.

3. **Rayleigh Channel:** Rayleigh multipath fading channel can be modeled by considering a flat fading channel with complex impulse response

$$\mathbf{h}(\mathbf{t}) = \mathbf{h}_i(\mathbf{t}) + j\mathbf{h}_q(\mathbf{t}) \quad (2.15)$$

Where $\mathbf{h}_i(\mathbf{t})$ and $\mathbf{h}_q(\mathbf{t})$ are zero mean Gaussian distributed, then the fading envelope is Rayleigh distributed and is given by (Kumar *et al.*, 2013):

$$h(\mathbf{t}) = \sqrt{|\mathbf{h}_i(\mathbf{t})|^2 + |\mathbf{h}_q(\mathbf{t})|^2} \quad (2.16)$$

The amplitude response of the Rayleigh fading multipath has Probability Density Function (PDF) given by (Awon *et al.*, 2012):

$$f(z) = \frac{2z}{\sigma^2} \exp\left(-\frac{z^2}{\sigma^2}\right), \text{ where } \sigma^2 = E[|\mathbf{h}(\mathbf{t})|^2] \quad (2.17)$$

The random process of flat Rayleigh fading with N multipath can be simulated with the sum-of sinusoid method described as in equation (2.14).

4. **Rician Channel:** Modelling Rician fading is similar to that of Rayleigh fading, except that in Rician fading a strong dominant component, LOS path exists between the transmitter and receiver. This can be modeled by using Gaussian random variables, one with zero mean and the other with non-zero mean. Consider two Gaussian random variables $X \sim N(m_1, \sigma^2)$ and $Y \sim N(m_2, \sigma^2)$, m_1 and m_2 are the means of the distributions and σ^2 is the variance (Viswanathan, 2013).

The impulse response can be modelled as a complex Gaussian random variable as (Kumar *et al.*, 2013):

$$Z = X + jY \quad (2.18)$$

Now the envelope of the complex random variable is given as (Kumar *et al.*, 2013):

$$R = \sqrt{X^2 + Y^2} \quad (2.19)$$

And the phase is given by (Kumar *et al.*, 2013):

$$\varphi = \tan^{-1} \frac{Y}{X} \quad (2.20)$$

Since, the two variables X and Y have different “means”, a non-centrality parameter (indicating the non-central mean) is defined as (Kumar *et al.*, 2013):

$$S = \sqrt{m_1^2 + m_2^2} \quad (2.21)$$

The non-centrality parameter (the imbalance in the means) is caused by the presence of dominant path in a Rician Fading environment. Due to this, the Rician K factor representing the ratio of power of Line-Of-Sight (LOS) and the power of Non-Line-Of-Sight (NLOS) is defined as (Viswanathan, 2013):

$$K = \frac{\text{Power of LOS component}}{\text{Power of NLOS components}} \quad (2.22)$$

This can be represented statistically as the power in the faded envelope that has been produced by the means of X and Y as(Viswanathan, 2013):

$$K = \frac{m_1^2 + m_2^2}{2\sigma^2} = \frac{S^2}{2\sigma^2} \quad (2.23)$$

The PDF of the envelope R with Rician distribution is given as(Awon *et al.*, 2012):

$$f_R(r) = \frac{r}{\sigma^2} \exp\left(-\frac{r^2 + S^2}{2\sigma^2}\right) I_0\left(\frac{r^2}{\sigma^2}\right) \quad (2.24)$$

Then, the random process of Rician fading with N multipath can also be simulated with the sum-of-sinusoid method described as in equation (2.14).

2.2.12 Performance Metrics

The following are some of the performance metrics of interest:

1. **Probability of False Alarm (PFA):**The probability of false alarm is a measure of how many times the CR has identified the presence of a primary user in a channel whereas it does not exist. This is important from a secondary user perspective as it leads to losing transmission opportunity.
2. **Probability of Missed Detection (PMD):**The probability of missed detection is a measure of how many times the secondary user failed to detect the primary user. This is important from a secondary user perspective as it indicates how many times the CR fails to identify the presence of a primary user, while actually it does exist which will cause interference on the primary user's transmission.
3. **Signal to Noise Ratio:**SNR is important from a comparison point of view and explains the behavior of the spectrum sensing tool under varying noise conditions at specific receiver sensitivity. Most often this is measured at the output of the receiver.

2.3 Review of Similar Works

There have been several related research works and the following is a review of some of the more pertinent ones:

Javed and Mahmood (2010) introduced the concept of time-frequency analysis into energy detection based spectrum sensing technique. This technique was used to localize a transmission signal in both time and frequency domains in cognitive radio simultaneously, in order to achieve a better estimation of the energy spectral density of the signal, thereby enabling the determination of a better sensing threshold. The researchers used Wigner-Ville distribution for localizing digital TV band frequency in time and frequency domains simultaneously. They were able to set a better sensing threshold. The major limitation encountered was that the Wigner-Ville distribution had weak performance when the spectrum been sensed was multicomponent. It suffered from cross terms or cross component that caused smearing of the signal in frequency domain based analysis and thereby causing a problem in the readability of the resulting distribution. These cross terms existed between the signal and the noise resulting in increased amplitude of the noise floor in the timefrequency distribution at instances where actual amplitudes were less. In order to minimize the effect of cross component the researcher chose a delay factor such that the signal of analysis appear mono component, this delay factor acted as smoothing function along the time domain which again led to poor frequency resolution.

Dikmese *et al.*, (2011) investigated spectrum sensing for a CRoperating in the unlicensed ISM band at 2.4GHz, a scenario where only Cyclic Prefix Orthogonal Frequency Division Multiplexing (CP-OFDM) based 802.11g WLANsare present was considered. The performance of Fast Fourier Transform (FFT) and Analysis Filter Bank (AFB) in analyzing the radio scene consisting of WLANsignals were considered. One important problem was that users operating in

the same radio environment might cause significant interferences to each other. For the multitude of systems operating in the ISM bands, no effective coordination or Radio Resource Management (RRM) functions existed, which led to inefficient utilization of these frequency bands. As a spectrum sensing method, AFB had some benefits due to better spectral containment of the sub-bands. The spectral containment depended greatly on the prototype filter design. However, there was a trade-off between spectral resolution and implementation complexity. A filter bank of 50 dB stopband attenuation and modeled WLAN signal as a zero-mean Gaussian variable. The absolute square of FFT or AFB output was then compared with a threshold value which was determined according to the assumed noise variance and desired false alarm probability they set to detect a primary signal at a certain frequency. Smoothing was also done on the FFT or AFB output, a two-dimensional time-frequency window was implemented for smoothing of the spectrum estimates and rectangular filter window was applied. The problem with FFT was that, it could only localize the signal in frequency domain which means information about time would be lost and no clear information of the power spectral density of the signal with time could be gotten. Furthermore, the AFB required many filters which might have taken much time than desired for the sensing period.

Bektas *et al.*, (2012) presented a spectrum sensing algorithm based on calculation of energy in sub-bands of the communication signal using wavelet transform while trying to maintain a low computational complexity. An attempt was made to achieve a multiresolution analysis feature of the signal by using scaled and shifted in time wavelet functions using base wavelet function called mother wavelet function. The work assumed the wavelet transform as filter-bank analysis. Signal was applied to High Pass Filters (HPF) and Low Pass Filters (LPF) so that detailed and approximation wavelet coefficients were obtained, respectively for each filter on the same

band. Cut-off frequency of $\pi/2$ was chosen for the first set of filters and divided by two at each level as scaling factor. Wavelet coefficients obtained for each scale denoted behavior of signal in the frequency band and total energy of the wavelet coefficients in the band was calculated and the primary user detected. The researchers subjected their proposed technique to Additive White Gaussian Noise (AWGN) only while varying the Signal to Noise Ratio (SNR) between -1 to -10dB. The consequence of using two filters at the same time in each sub-band was an increased computational complexity compared to the conventional energy detector. Also, subjecting the work to AWGN only is not enough as a fading channel would experience some more complex noise. The SNR could also have been tested over a wider range of SNR with lower values to affirm the performance of the work.

Javed *et al.*, (2012) proposed radio mode identification which enabled the cognitive radio to identify various useful parameters of primary user transmission such as modulation scheme, transmission technology, frame size and multiplexing technique, etc which could be utilized by the cognitive radio for optimizing spectrum sensing. This technique used instantaneous frequency and delay spread obtained through time frequency analysis. Pseudo-Wigner Distribution (PWD) was used and the resulting time-frequency distribution was subjected to thresholding against a set sensing threshold. The sensing threshold was selected by assuming two overlapping distribution of signal and noise power probability density functions. The effects of noise were reduced from the resulting binary image by performing image morphing. The image was then scanned vertically and horizontally to identify the locations of the individual peaks. The features of the modulation schemes that were identified were instantaneous frequency, bandwidth, occupation time and duration of occupation of each occupied slot. Based on all the parameters identified, an estimate of the type of modulation scheme was made and decision that

whether the spectrum users were licensed primary users or competing secondary users were also made. The sensing was carried out with SNR values changing from -45 to 0dB. The simulation assumed an AWGN noise. The cross terms are minimized by selecting the observation window so as to keep the received signal mono-component. The performance of the algorithm was tested with different users, more accuracy was gotten for Frequency Hop Spread Spectrum (FHSS) primary user in comparison to Orthogonal Frequency Division Multiplexing (OFDM) primary user. This was because of the difficulties in differentiating the low amplitude wide band signal from the background noise at low SNR values. The work achieved a good sensing accuracy but at the expense of increased computational complexity owing to additional image scanning and morphing for feature identification.

Guibene *et al.*, (2012) proposed an algebraic detection-based spectrum sensing approach. The technique was based on Short Time Fourier Transform (STFT) using sliding window. The work considered time and frequency features of the sensed signals and focused on the intensity. It assumed the effect of a primary user as a polynomial of the N th order, and the proposed algebraic detection required a filter bank of N filters. The work derived from the approach of Wavelet Transform (WVT), where spectral analysis was performed in two dimensions by considering algebraic properties of channel occupation and employing several filters in order to estimate the spectral power density of the signal of analysis. Consequently, the requirement of N filters increased the computational complexity and also the time taken to sense the signal increases even though the number of samples taken per filter were considerably small.

Monfared *et al.*, (2013) applied compressive sampling technique to the existing time-frequency distribution so that the number of samples required to be processed and reconstructed would be small leading to a reduced sensing time. The researchers applied another time-frequency

technique; the pseudo Wigner-Ville distribution in order to compensate for the effect of cross terms in the original Wigner-Ville distribution (WVD). The result obtained was an improved accuracy in sensing the signal energy and the reduced time in sensing owing to reduced samples. Compressed sensing takes advantage of the redundancy in signals (they are not pure noise). In particular, many signals are sparse, that is, they contain many coefficients close to or equal to zero, when represented in some domain. This was the same insight used in many forms of lossy compression. The methods of signal reconstruction in compressive sensing were extremely slow and returned a not so perfect reconstruction of the signal. Pseudo Wigner-Ville distribution (PWVD) is not without its own shortcomings as it is not completely free of cross terms and there are other distribution techniques that might perform better than it such as Levin distribution or Rihaczek distribution.

Hamid *et al.*, (2013) worked on blind spectrum sensing using a technique called discriminant analysis. This is an extension of the work carried out by the same group of researchers in 2012 and extended with a technique called Primary User (PU) peel-off in 2013. The main idea of discriminant analysis was to partition the signal in two groups (the noise only group and the PU signal plus noise group) such that the groups' means are maximally separated under the constraint that the variance within each group is as small as possible. The discriminant analysis was applied to a received signal that contains a PU signal and noise, the boundary between the two groups, the noise only group and the PU signal plus noise group were measured as the discrimination height and an average energy calculated. If this calculated average exceeds the average energy of the spectral lines in the noise group, then a PU signal is present. Issues were encountered when only noise was applied to the test statistic. Since noise cannot be absolutely flat, a discrimination height will be selected and the two groups discriminated. The peel-off technique was introduced

to solve this problem which was explained with the assumption that the sensed spectrum contains two PUs, one with a large SNR and the other with small SNR, since the discriminator groups signal in to two then, it will consider the weak PU as noise and will no longer be able to detect it because weak PU will be discriminated in the noisegroup. The peel-off technique detected all primary users based on an iterative algorithm. The stopping criterion for the iterative algorithm critically depends on a threshold selection which the work did not consider.

Biagi *et al.*, (2014) proposed access policy that handled spectrum sensing by means of the Wigner–Ville transform (WVT). The researchers analyzed the time and frequency features of the received interference, and represented them on a time–frequency grid as an image in which brightness reveals the spectrum occupancy. In order to test the access scheme in a realistic scenario, a test bed was set up, Wigner–Ville Cognitive Radio Access (WiVCoRA) based on Virtex 4 field-programmable gate array (FPGA). A packet-oriented wireless network was considered, where a secondary transmitter belonging to set of SUs attempts to access the shared medium to establish a connection with its intended receiver. An assumption was made that, among secondary nodes, there exists a time hierarchy, associated to node i is access request time t_i , and to node $i + 1$, time t_{i+1} (and so forth) with $t_{i+1} > t_i$, which means that the i th node will access before the $i + 1$ node, provided that sufficient resources are available for its connection. This assumption may not be realistic as SUs considering a non-cooperative sensing would not depend on each other to sense and access a spectrum hole. WVT approach was used, where the spectral analysis was performed in two dimensions by applying some algebraic properties of the occupation and referring to several filters to be used. Their work focused more on the interference profile than in its simple power amount, they further processed WVT image so as to show the spectrum occupancy. In order to trace the interference profile that is in the image, an

edge detection technique was applied to the grayscale image derived by the WVT but, research has shown that WVT suffers from cross terms and the edge detection applied added to the complexity as further filtering is required with N filters depending on number of sub-bands as edge detection divides a frequency band of analysis into sub-bands.

Hiremath *et al.*, (2015) investigated spectrum sensing by applying S-Method based joint time frequency analysis which is a combination of the strengths of Short Time Fourier Transform (STFT) and Wigner-Ville distribution (WVD). It was identified that WVD has better time-frequency resolution but suffers from cross terms and STFT does not suffer from the same. The Short Time Fourier Transform (STFT) is simply a conventional energy detector using rectangular time window. As there are various types of windowing techniques, literature has shown that rectangular window is not the best and it could be suggested that the window should be changed for better filtering of the signal. The work hybridized the two techniques to get a better trade-off between accuracy and sensing time but clearly there are other time-frequency analysis techniques that can outperform WVD and STFT combination as they handle the issue of cross terms better. Also the hybridization may lead to computational complexity which is not desirable.

Paul *et al.*, (2015) proposed a wavelet based spectrum sensing approach to detect the active sub-bands within a licensed band. An exponential moving average based multi-scale sum (EMAMS) spectrum sensing approach was devised to decompose the power spectral density (PSD) signal and extract the edges of signals, by assigning exponentially changing weights to the different scales of the wavelet transform to detect which sub-bands are active or signals with unpredictable start and end frequencies. Each signal has a start frequency and an end frequency, which were called edges of the signal. The objective of edge detection of spectrum sensing was to detect the start and the end frequency of each signal. Edges were detected in two stages by using

power threshold and bandwidth threshold. At the higher scale, existence of signals were detected, but could not find the accurate start and end frequencies of the signals, as they are shifted. Most of existing work on signal edge detection used the multi-scale product which multiplies the wavelet transform results at two adjacent scales, but this approach fixed a threshold constant and a weighting factor at 20 and 0.5 respectively, the basis of which was not established neither in literature nor the work.

Berbra *et al.*, 2016 proposed a fast spectrum sensing approach based on using observed samples during a window with length of K OFDM symbols. They computed number of subcarriers N_d , and cyclic prefix length, N_c values of the real part of the autocorrelation function of the signal at time lag, N_d . These values correlation bins, correspond to one period of the autocorrelation function. The output of the correlator representing the correlation bins are sent serially into a shift register of length $N_c + N_d$. The $N_c + N_d$ cells were then ranked in an ascending order according to their magnitude and a test statistic was formed from the upper bound value, while the other lower values were used to form an estimate of the background noise level, this required a dedicated hardware. The estimate is then multiplied by a constant threshold multiplier, which was selected so as to achieve a desired false alarm probability. Their work achieved a good sensing threshold but at the cost of implementation due to computational complexity.

Based on the literature reviewed, many researchers had proposed different methods on energy detection technique for spectrum sensing. The works attempted to determine optimum detection threshold with different levels of compromise on the computational complexity, sensing time and accuracy. Determination of detection threshold is affected by the amount of noise present in the channel. This means that a good knowledge of the amount of noise present in a particular spectrum band of interest is required. The use of time-frequency analysis has shown a great

potential in this regard. There are several other distribution techniques under the time-frequency analysis that can still be explored in order to combat the effect of cross terms which affects the accurate determination of detection threshold. A smoothed pseudo Wigner-Ville distribution is proposed because of its high efficiency in suppressing cross term as compared with other candidate techniques. The proposed technique will be compared using the performance metrics established in literature, with the work of Monfared et al., (2013), which furthered the work of Javed and Mahmood, 2013 by applying Pseudo Wigner-Ville Distribution.

CHAPTER THREE

MATERIALS AND METHODS

3.1 Introduction

This chapter describe in detail the process of OFDM signal generation, Hilbert transforming the generated signal, application of smoothed pseudo Wigner-Ville distribution in order to calculate the energy spectral density required in the setting of threshold and the likelihood ratio test to check the performance of the set threshold.

3.2 System Model (spectrum sensing scenario)

A non-cooperative single secondary user was considered for this work. The scenario depicted a single secondary user scanning for spectrum holes opportunity at a target primary user band. This was done with the assumption that if spectrum sensing operation achieved a high percentage of detection and a low false alarm, it could be implemented on several cognitive radios scanning for spectrum holes in different bands or implementing the same technique in the same band in a

cooperative manner for better efficiency across the space in a geographical location. The model is represented in Figure 3.1.

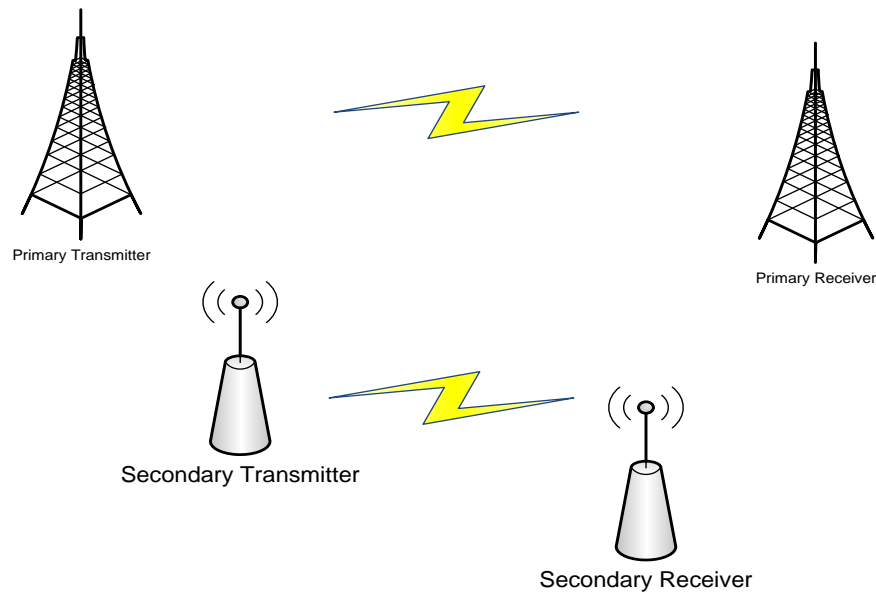


Figure 3.1 Spectrum sensing scenario for a primary user and secondary user

3.3 Signal Simulation Process

OFDM data were modulated to time signal so that all carriers transmit in parallel to fully occupy the available frequency bandwidth. OFDM data were generated by taking symbols in the spectral space using modulation techniques such as *M*-ary phase shift keying (*M*-PSK), quadrature amplitude modulation (QAM), etc, and converted the spectra to time domain by taking the inverse discrete Fourier transform (IDFT) or inverse fast Fourier transform (IFFT). The latter was adopted in this work due to its effectiveness. OFDM symbols are typically divided into frames, so that the data were modulated frame by frame in order for the received signal be in synchronization with the receiver. The number of carriers in an OFDM system is determined by the available bandwidth and by the IFFT size. The relationship is described by (Ingram *et al.*, 2000):

$$\text{number of carrier} \leq \frac{\text{ifft size}}{2} - 2$$

The choice of the modulation technique varies with the data rate and bit error rate (BER). The higher the order of the modulation technique, the larger the symbol size, thus the less the number of symbols needed to be transmitted, and the higher the data rate achieved.

A bitmap grayscale image was used in this work, it was converted to a baseband signal, modulated and transmitted through the communication channel modeled under three different channel conditions of AWGN, Rayleigh, and Rician. The expression for one OFDM symbol starting at $t = t_s$ is given as (Ingram *et al.*, 2000):

$$S(t) = \text{Re} \left\{ \sum_{i=-\frac{N_s}{2}}^{\frac{N_s}{2}-1} d_{i+\frac{N_s}{2}} \exp \left(j2\pi \left(f_c - \frac{i+0.5}{T} \right) (t - t_s) \right) \right\}, t_s \leq t \leq t_s + T \quad (3.1)$$

where d_i are complex modulation symbols, i is the OFDM symbol number, N_s is the number of subcarriers, T the symbol duration, and f_c the carrier frequency.

The OFDM signal was generated using Matlab through the following processes:

1. **Serial to parallel conversion:** The input image was first converted to serial data stream which was then formatted into word sizes or symbols depending on the modulation format chosen and then shifted to parallel format. This was then transmitted in parallel by assigning each symbols to carriers.
2. **Data modulation:** The data to be transmitted on each carrier was differentially encoded with previous symbols, then mapped into a Phase Shift Keying (PSK) format. Differential encoding requires an initial phase reference an extra symbol was added at the start for this purpose. The data on each symbol was then mapped to a phase angle based on the modulation method. For example, for QPSK the phase angles used are 0, 90, 180, and

270 degrees. The use of phase shift keying produces a constant amplitude signal and was chosen for its simplicity and its robustness against amplitude fluctuation due to fading.

3. **Inverse Fourier Transform:** After the required spectrum is worked out, an Inverse Fourier Transform was used to find the corresponding time waveform. The guard period was then added to the start of each symbol.
4. **Addition of Guard Period:** The guard period is a cyclic extension of the symbol to be transmitted. This was done to allow for symbol timing to be easily recovered by envelope detection and also to reduce inter-symbol interference.

After the guard has been added, the symbols were then converted back to a serial time waveform. This is the base band signal for the OFDM transmission and was transmitted through AWGN and multipath channels (Raleigh and Rician). The complete program code for the OFDM user signal simulation is found in Appendices A to F.

3.3.1 AWGN Channel

AWGN is a type of noise which exists in the communication channels generally. In an AWGN channel model, we always assume that there is no any other distortion or effects from other sources. AWGN is a model for the thermal noise generated by random electron movement in the receiver.

3.3.2 Rayleigh Channel

The Rayleigh distribution was used to model the amplitude and phase of multipath fading signal when no line of sight (LOS) path exists in between transmitter and receiver, but only have indirect path than the resultant signal received at the receiver will be the sum of all the reflected and scattered waves. In this work, three paths were assumed.

3.3.3 Rician Channel

It occurs when there is a LOS as well as non-LOS path in between the transmitter and receiver, i.e. the received signal comprises of both the direct and scattered multipath waves. In this channel, the LOS path has a dominant signal than others and the ratio of the signal strength between this path and other part is known as the K-factor. Three paths were assumed with a LOS path and two multipath for the modelling of this channel in this work.

OFDM signal transmission simulation parameters: Table 3.1 summarizes the parameters used for the simulation of the OFDM signal transmission.

Table 3.1 OFDMSimulation Parameters

Parameters	Values
Source data	Gray scale image with different sizes (800 by 600, 600 by 800, 400 by 300)
IFFT size	2048
Number of carriers	Defined by $(number\ of\ carrier \leq \frac{ifft\ size}{2} - 2)$.
Modulation method	Varied between BPSK, QPSK, 16PSK, 256PSK
Amplitude power clipping (dB)	3 – 9
Signal to Noise Ratio (dB)	Varied between -45 to 0

3.4 Hilbert Transforming the SimulatedSignal

The purpose of Hilbert transforming the generated signal is to get the analytic associate of it. An analytic signal is derived from a real signal, a signal is real, if it exhibits Hermitian symmetry between positive and negative components allowing the negative components to be deduced from the positive components. This enables the elimination of the negative components without losing information and gives the benefit of halving the bandwidth requirement.

Generally, analytic signals in the time domain can be represented as (Smith, 2007):

$$s(t) = \frac{1}{2\pi} \int_0^{\infty} S(\omega) e^{j\omega t} d\omega \quad (3.2)$$

where $S(\omega)$ is a complex conjugate setting the amplitude and phase of the positive frequency complex sinusoid $e^{j\omega t}$ at frequency ω .

Any real sinusoid $Z\cos(\omega t + \phi)$ can be converted to a positive frequency complex sinusoid $Ze^{j(\omega t + \phi)}$ by shifting it a quarter cycle time-shift to generate a quadrature phase component $Z\sin(\omega t + \phi)$ as the imaginary part(Boashash, 2015).

$$Ze^{j(\omega t + \phi)} = Z\cos(\omega t + \phi) + jZ\sin(\omega t + \phi) \quad (3.3)$$

The Hilbert transform is realized as a filter that shifts each sinusoidal component of the real signal by a quarter cycle. It introduces a phase shift of $-\frac{\pi}{2}$ at each positive frequency component and $+\frac{\pi}{2}$ at each negative frequency component. The Hilbert transform is given as(Boashash, 2015):

$$s(t) = z(t) + jH(t) \quad (3.4)$$

where $s(t)$ is the analytic signal and has all the negative frequencies filtered out, $z(t)$ is the real signal and $jH(t)$ is the imaginary part of the real signal $s(t)$.

The realization of the Hilbert transform process is illustrated below:

$x(t)$ is represented in its positive and negative frequency components at a particular frequency ω_0 as follow (Smith, 2007);

$$x_+(t) = e^{j\omega_0 t} \text{ and } x_-(t) = e^{-j\omega_0 t} \quad (3.5)$$

Applying a quarter cycle shift of $-\frac{\pi}{2}$ at positive frequency component and $+\frac{\pi}{2}$ at negative frequency component gives:

$$y_+(t) = e^{-j\frac{\pi}{2}} e^{j\omega_0 t} = -je^{j\omega_0 t} \quad (3.6)$$

$$y_-(t) = e^{j\frac{\pi}{2}} e^{-j\omega_0 t} = je^{j\omega_0 t} \quad (3.7)$$

Adding the resulting components together to get the analytic signal gives:

$$s_+(t) = x_+(t) + jy_+(t) = e^{j\omega_0 t} + (-j^2 e^{j\omega_0 t}) = 2e^{j\omega_0 t} \quad (3.8)$$

$$s_-(t) = x_-(t) + jy_-(t) = e^{-j\omega_0 t} + (-j^2 e^{-j\omega_0 t}) = 0 \quad (3.9)$$

The result $s_-(t)$ explained how the negative frequency component is filtered out and the positive frequency component gain increased. This is the same way negative frequency is removed in all real signal by applying the Hilbert transform on them. A real signal case is depicted below (Smith, 2007):

$x(t)$ is a real signal which equals $2\cos(\omega_0 t)$, by Euler's identity

$$x(t) = 2\cos(\omega_0 t) = e^{j\omega_0 t} + e^{-j\omega_0 t} \quad (3.10)$$

Applying Hilbert transform (adding phase shift of -90 and +90)

$$y(t) = e^{j\omega_0 t - j\frac{\pi}{2}} + e^{-j\omega_0 t + j\frac{\pi}{2}} \quad (3.11)$$

$$= -je^{j\omega_0 t} + je^{-j\omega_0 t} = 2\sin(\omega_0 t) \quad (3.12)$$

The analytic signal $s(t)$ becomes:

$$s(t) = x(t) + jy(t) \quad (3.13)$$

$$= 2\cos(\omega_0 t) + j2\sin(\omega_0 t) = 2e^{j\omega_0 t} \quad (3.14)$$

Generally, the process of Hilbert transform is as summarized (Boashash, 2015):

- 1 The Fourier transform of the signal will be taken
- 2 Phase lag of $+\frac{\pi}{2}$ and $-\frac{\pi}{2}$ is introduced to the positive and negative frequency components
- 3 Inverse Fourier transform is taken

This is the process by which the generated signal was Hilbert transformed to get the analytic associate before subjecting to further processing.

3.5 Smoothing and Calculating the Energy Spectral Density of the Received Signal Using SPWVD

The analytic signal that resulted from the process described in section 3.4 above was processed using Smoothed Pseudo Wigner-Ville Distribution of the time-frequency tool box where the cross-terms are been suppressed without compromising poor resolution. This distribution is as given in the following equation based on equation (2.12)(Auger *et al.*, 2005):

$$SPWVD_x(t, \nu) = \int_{-\infty}^{\infty} h(\tau) \int_{-\infty}^{\infty} g(\nu - t) s(t + \frac{\tau}{2}) s^*(t - \frac{\tau}{2}) ds e^{-j2\pi\nu\tau} d\tau$$

where:

't' is the time of occurrence of signal 's'

' τ ' is a delay in time or time shift

' ν ' is the frequency shift or Doppler shift

$h(t)$ and $g(s - t)$ are the separate smoothing functions along the time and frequency domains respectively.

The smoothing was performed on the distribution by adjusting the window width of the smoothing window $h(t)$ and $g(s - t)$ separately till the cross-terms are suppressed and good resolution achieved.

Since we desire good resolutions too and not just cross term suppression, the Kaiser-Bessel window was used for the smoothing window $h(t)$ and its beta parameter used was 7 to reduce the effects of side lobes and the window length M of 79 was used to achieve a clear distinction between closely packed frequencies of the signal in the frequency plane. The Blackman window

was used for the smoothing window $g(s - t)$ with window length M of 33 gave a satisfactory cross-terms suppression in the time plane.

The energy spectral density of the smoothed distribution was extracted using the marginal time-frequency function of the time-frequency tool box. The energy spectral densities were extracted as (Auger *et al*, 2005):

$$E = \int_{-\infty}^{+\infty} \int_{-\infty}^{+\infty} tfr(t, f) df dt \quad (3.15)$$

where

E represents the energy spectral density of the distribution

tfr represents the Smoothed Pseudo Wigner-Ville distribution function

t represents the vector containing time sample in seconds

f represents the vector containing frequency samples in hertz

The respective MATLAB codes for smoothening and calculating energy spectral densities of the simulated signals are as shown below:

MATLAB code for implementing PWVD

```
Ev=[];
for k = 0:1:99;
realSig = OFDM_SIM(n); % n is the variable for SNR
newSig = hilbert(realSig);
sig=newSig;
h=tfib_window(79, 'Kaiser'); %calling window
[tfr,t,f] = tfrpwv(sig',1:1024,127,g,h,1); %applying PWVD
[margt,margf,E]=margtfr(tfr,t,f);
Ev=[Ev, E]; % getting out the Energy Value
end
```

MATLAB code for implementing SPWVD

```
Ev=[];
for k = 0:1:99;
```

```

realSig = OFDM_SIM(n); % n is the variable for SNR
newSig = hilbert(realSig);
sig=newSig;
g=tfib_window(33,'Blackman'); h=tfib_window(79,'Kaiser'); % calling window
[tfr,t,f] = tfrspwv(sig',1:1024,127,g,h,1); % applying SPWVD
[margt,margf,E]=margtfr(tfr,t,f);
Ev=[Ev, E]; % getting out the Energy Value
end

```

3.6 Threshold Determination

The threshold for the spectrum sensing based on the Smoothed Pseudo Wigner-Ville distribution time-frequency analysis were set after a hundred simulations was done following the processes above. The threshold was calculated as an average of the energy spectral densities gotten from the analysis of the generated signals at a target SNR and for the three modelled channel conditions. The mean energy density was taken as threshold for each of the channels. Target SNR of -25dB was used to determine the threshold because the standardization body specified that, the detection threshold for energy detection that can detect reliably at a received power of -116dBm at the receiver is required below which reliable detection is not guaranteed (IEEE 802.22.a-2014, 2014). This translates to a SNR of -25dB and the energy spectral densities at -25dB after one hundred simulations were averaged in order to estimate and determine the threshold.

3.7 Generalized Likelihood Ratio Test (GLRT) on the Set Threshold

The value of the threshold estimated would not convey a significant meaning on its own whether there is improvement on the missed detection probability and false alarm probability therefore, it is necessary to subject the threshold to performance test. The GLRT was carried out in order to ascertain the improvement achieved on the sensing threshold by comparing the energy spectral

densities of a new simulated signals subjected to the same channel conditions as the model signal. A hundred simulations and measurements are taken at each SNR from 0dB to -45dB. As it has already been discussed in section 2.2.4 under the sub-heading energy detection, the goal of spectrum sensing is to decide between two hypothesis H_0 and H_1 where H_0 represents the decision the sensed band is unoccupied and H_1 represents the decision that the sensed band is occupied.

3.8 Performance Metrics

The performance metrics used to evaluate the performance of the set threshold using SPWVD are as explained below:

3.8.1 Probability of False Alarm (PFA): The probability of false alarm is a measure of how many times the cognitive radio has identified the presence of a primary user in a channel whereas it does not exist. This is important from a secondary user perspective as it leads to losing transmission opportunity and it is given by (Atapattu *et al.*, 2014):

$$PFA = P[E > T | H_N] \quad (3.16) \text{ where:}$$

E is the detected energy

T is the set threshold

H_N is the condition that there is no transmission ongoing.

The simulation was repeated for hundred times and each time, a new value is gotten for E at a fixed SNR value. Then, the PFA is expressed as (Lopez-Benitez & Casadevall, 2013):

$$PFA = P(H_1 | H_0) \quad (3.17)$$

where H_1 denotes the decision that the E is greater than the threshold when there is no transmission ongoing and H_0 denotes the decision that the E is less than the threshold when there is no transmission ongoing.

This scenario of PFA was treated using conditional probability as:

$$P(H_1|H_0) = \frac{P(H_1 \cap H_0)}{P(H_0)} \quad (3.18)$$

where $P(H_1 \cap H_0)$ is the case where the detected E is equal to the threshold and denoted by H_E . The E for each simulation of the hundred simulations were compared with the set threshold and the respective counts of H_1 , H_0 and H_E were taken and substituted into the conditional probability to get the PFA.

3.8.2 Probability of Missed Detection (PMD):The probability of missed detection is a measure of missed spectrum holes opportunities. This is important from a secondary user perspective as it indicates how many times the CR fails to identify the presence of a primary user, while actually it does exist and this will lead to interference on the primary user's transmission. The PMD is given as (Atapattu *et al.*, 2014):

$$\text{PMD} = P[E < T|H_T] \quad (3.19)$$

where:

H_T is the condition that there is transmission ongoing.

The simulation was repeated for hundred times as well and each time, a new value is gotten for E at a fixed SNR value. Then, the PMD is expressed as (Lopez-Benitez & Casadevall, 2013):

$$\text{PMD} = P(H_0|H_1) \quad (3.20)$$

where H_0 denotes the decision that the E is less than the threshold when transmission is ongoing and H_1 denotes the decision that the E is greater than the threshold when there is transmission ongoing. This scenario of PMD was treated using conditional probability given as:

$$P(H_0|H_1) = \frac{P(H_0 \cap H_1)}{P(H_1)} \quad (3.21)$$

This $P(H_0 \cap H_1)$ is the case where E is equal to the threshold and denoted by H_E . The E detected for each simulation of the hundred simulations were compared with the set threshold and the respective counts of H_1 , H_0 and H_E were taken and substituted into the conditional probability of equation (3.20) to get the PMD.

3.8.3 Signal to Noise Ratio (SNR): This is the ratio of the signal power to noise power. It is important from a comparison point of view and explains the behavior of the spectrum sensing tool under varying noise conditions. Most often this is measured at the output of the receiver and it is given as (Brooker, 2008):

$$SNR = \frac{\text{Signal Power}}{\text{Noise Power}} \quad (3.22)$$

The values of the received SNR at the secondary user were varied from 0 to -45dB as in Monfared et al., 2013 so that the detected energies E can be used to calculate the PFA and PMD under the varying SNR for both the SPWVD and PWVD techniques.

3.8.4 Relationship between PFA, PMD and SNR: The relationship between these parameters is as explained as follows:

Equation (3.21) can be interpreted as (Brooker, 2008):

$$\frac{S}{N} = \frac{2E}{N_0} \quad (3.23)$$

$$E = \left(\frac{S}{N}\right) \frac{N_0}{2} \quad (3.24)$$

where

E is the received signal energy

S is the peak instantaneous signal power

N is the average noise power

N_0 is the single sided noise power density

Now, substituting equation (3.23) into (3.16) and (3.19) to get the respective PFA and PMD as follows:

$$\text{PFA} = P\left[\left(\frac{S}{N}\right) \frac{N_0}{2} > T | H_N\right] \quad (3.25)$$

$$\text{PMD} = P\left[\left(\frac{S}{N}\right) \frac{N_0}{2} < T | H_T\right] \quad (3.26)$$

The probability of H_1 knowing H_0 is the case of noise only transmission used for calculating the PFA using the values of the respective H_1 , H_0 and H_E gotten from equation (3.25) in the conditional probability of equation (3.18), while for the case of signal plus noise transmission, the PMD were calculated as probability of H_0 knowing H_1 using the values of the respective H_1 , H_0 and H_E gotten from equation (3.26) in conditional probability of equation (3.21). The respective PMDs and PFAs were tabulated and plotted for both SPWVD and PWVD and were discussed in the result and discussion chapter.

CHAPTER FOUR

RESULTS AND DISCUSSION

4.1 Introduction

This chapter presents the results obtained from the comparison of performance between the spectrum sensing thresholds gotten from the use of Smoothed Pseudo Wigner-Ville Distribution against the Pseudo Wigner-Ville Distribution. The results show the improvement achieved with the employed technic.

4.2 Results of the comparisons

The plots show the performance of the thresholds obtained from both the smoothed pseudo Wigner-Ville distribution (SPWVD) against the pseudo Wigner-Ville distribution (PWVD). The probabilities of missing detection were plotted against Signal to Noise Ratios (SNRs) and the probabilities of false alarm against SNRs for each channel condition modeled that is, AWGN, Rician and Rayleigh channels respectively.

Tables 4.1 to 4.6 present the data gotten from the various simulations done at different SNRs and the resulting counts of presence or absence of primary user signal. H_0 denotes the absence of primary use while H_1 denotes the presence of primary user. Also, the resulting probability of missed detection (PMD) and probability of false alarm (PFA) presented were obtained from the test statistics of equations (3.26) and (3.25) and then subjected to conditional probability of equations(3.20) and (3.17) as discussed in section 3.8.

The percentage reductions achieved using SPWVD over PVWD in both PMD and PFA were calculated and then averaged using:

$$\text{percentage reduction} = \frac{\text{PMD of PWVD} - \text{SPWVD}}{\text{PWVD}} \times 100 \quad (4.1)$$

$$\text{percentage reduction} = \frac{\text{PFA of PWVD} - \text{SPWVD}}{\text{PWVD}} \times 100 \quad (4.2)$$

Table 4.1 Data of SPWVD and PWVD with PMD for AWGN Channel

SNR (dB)	SPWVD				PWVD			
	H_0	H_1	H_e	PMD	H_0	H_1	H_e	PMD
-45	12	77	11	0.14	09	78	13	0.17
-40	07	82	11	0.13	12	76	12	0.16
-35	09	81	10	0.12	03	84	13	0.16
-30	09	76	13	0.12	05	83	12	0.15
-25	08	77	15	0.10	11	79	10	0.13
-20	06	79	15	0.08	11	79	09	0.11
-15	07	88	05	0.06	07	77	16	0.09
-10	09	86	05	0.06	07	83	10	0.08
-5	18	78	04	0.05	09	86	05	0.06
0	04	92	04	0.04	07	88	05	0.06

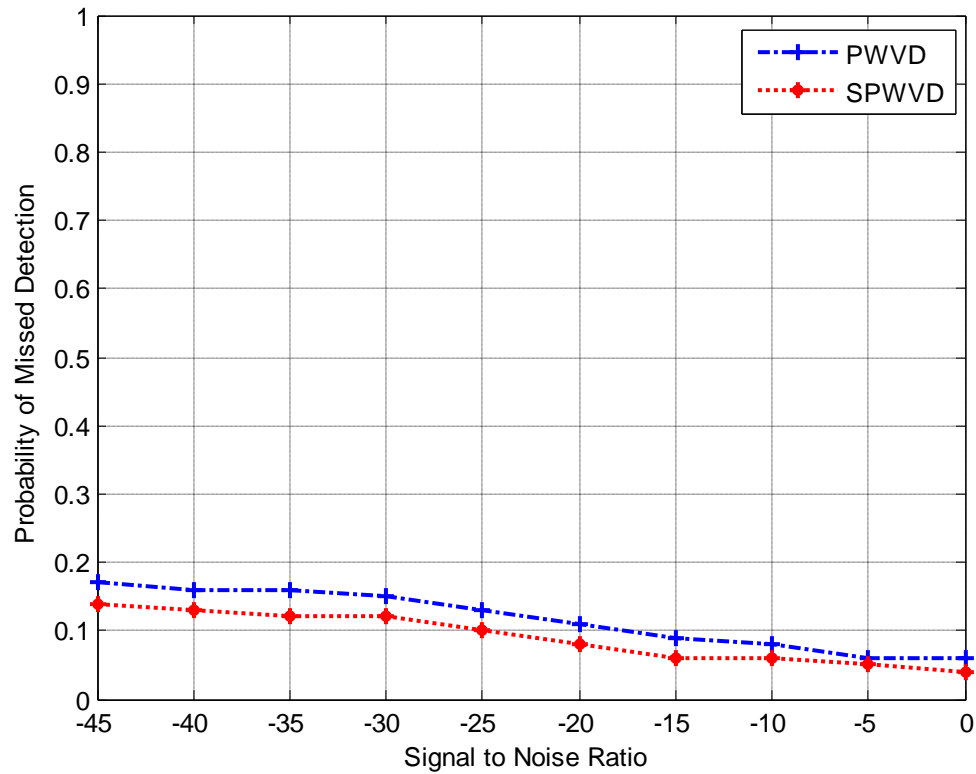


Figure 4.1 Plot of PMD against SNR for AWGN Channel

Figure 4.1 shows the plot of PMD of SPWVD and PWVD for AWGN channel against SNR. The plot was gotten from the values recorded in Table 4.1, the probabilities gotten for SPWVD are lower than those of PWVD and this is as a result of the further smoothening done in SPWVD. The performance of SPWVD over that of PWVD was 2.7% reduction in the PMD on an average.

Table 4.2 Data of SPWVD and PWVD with PFA for AWGN Channel

SNR (dB)	SPWVD				PWVD			
	H_0	H_1	H_e	PFA	H_0	H_1	H_e	PFA
-45	79	12	09	0.11	71	19	10	0.14
-40	86	05	09	0.11	73	17	10	0.14
-35	80	12	08	0.10	79	11	11	0.14
-30	81	12	07	0.09	76	15	09	0.12
-25	83	10	07	0.08	78	13	09	0.12
-20	79	15	06	0.08	79	12	09	0.11
-15	80	15	05	0.06	79	15	06	0.08
-10	92	04	04	0.04	80	15	05	0.06
-5	92	04	04	0.04	88	07	05	0.06
0	96	02	02	0.02	89	06	05	0.06

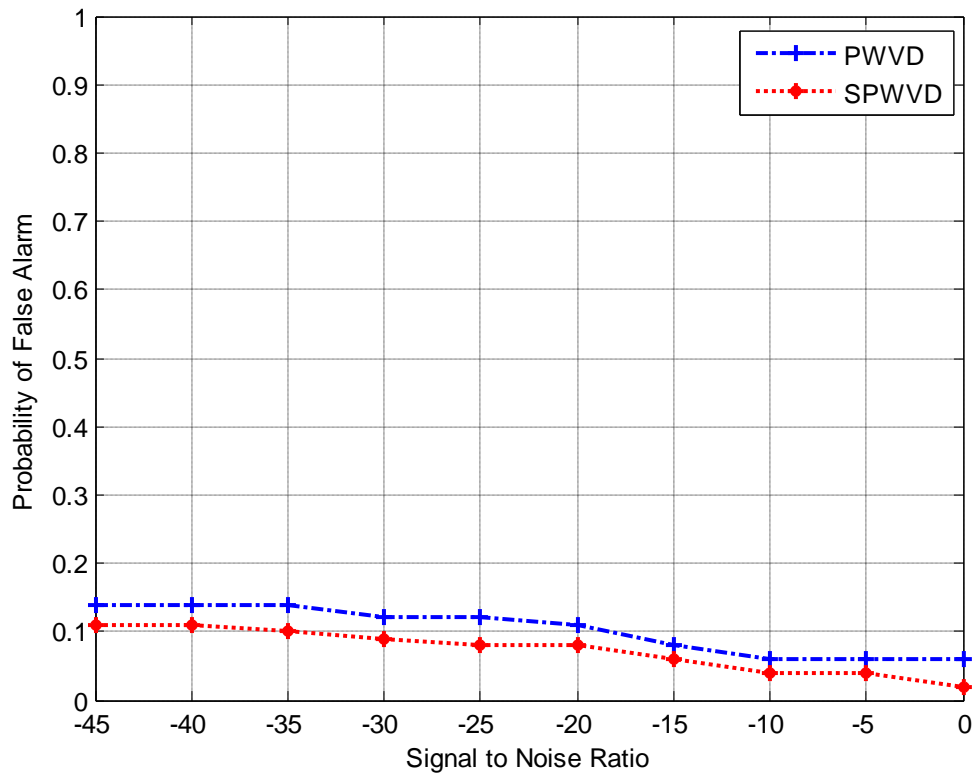


Figure 4.2 Plot of PFA against SNR for AWGN Channel

From Figure 4.2, the plot of PFA against SNR for SPWVD and PWVD are shown. The respective PFAs in SPWVD are lower than that of PWVD with 3% reduction in the PFA on an average. This is an improvement in performance of SPWVD over PWVD and it is as a result of further smoothing as earlier mentioned discussed under Figure 4.1.

Table 4.3 Data of SPWVD and PWVD with PMD for Rician Channel Condition

SNR (dB)	SPWVD				PWVD			
	H_0	H_1	H_e	PMD	H_0	H_1	H_e	PMD
-45	07	78	15	0.19	05	75	20	0.27
-40	09	77	14	0.18	10	72	18	0.25
-35	03	83	14	0.17	07	75	18	0.24
-30	08	79	13	0.17	09	74	17	0.23
-25	12	75	13	0.17	07	77	16	0.21
-20	07	80	13	0.16	06	79	15	0.19
-15	06	82	12	0.15	11	75	14	0.19
-10	08	80	12	0.15	05	81	14	0.18
-5	09	79	12	0.15	07	80	13	0.17
0	11	79	10	0.13	03	84	13	0.16

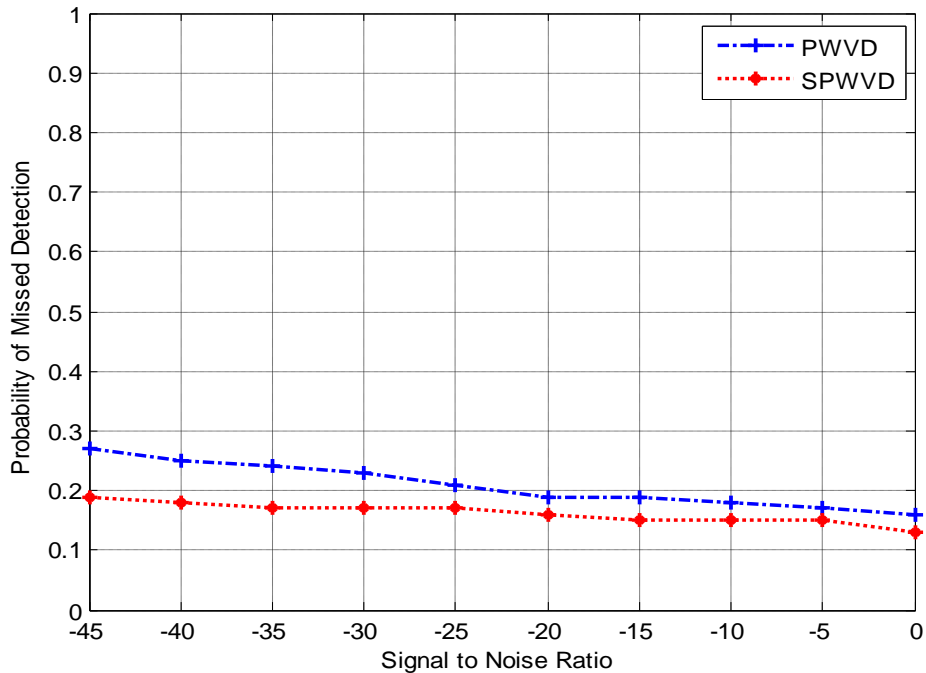


Figure 4.3 Plot of PMD against SNR for Ricain channel condition

From Figure 4.3, the PMD against SNR plots for SPWVD and PWVD are shown. The respective probabilities here for the Rician channel showed 4.7% reduction in PMD on an average. The performance of the SPWVD is better than that of PWV as the probabilities of missed detection are lower for the same SNR.

Table 4.4 Data of SPWVD and PWVD with PFA for Rician Channel Condition

SNR (dB)	SPWVD				PWVD			
	H_0	H_1	H_e	PFA	H_0	H_1	H_e	PFA
-45	80	10	10	0.13	64	24	12	0.19
-40	76	15	09	0.12	63	26	11	0.18
-35	78	13	09	0.12	71	16	13	0.18
-30	80	11	09	0.12	69	19	12	0.17
-25	81	09	10	0.12	73	14	13	0.17
-20	86	04	10	0.12	70	20	10	0.14
-15	79	12	09	0.10	72	18	10	0.14
-10	79	15	06	0.08	79	12	09	0.11
-5	78	17	05	0.05	83	10	07	0.08
0	79	16	05	0.05	85	10	05	0.06

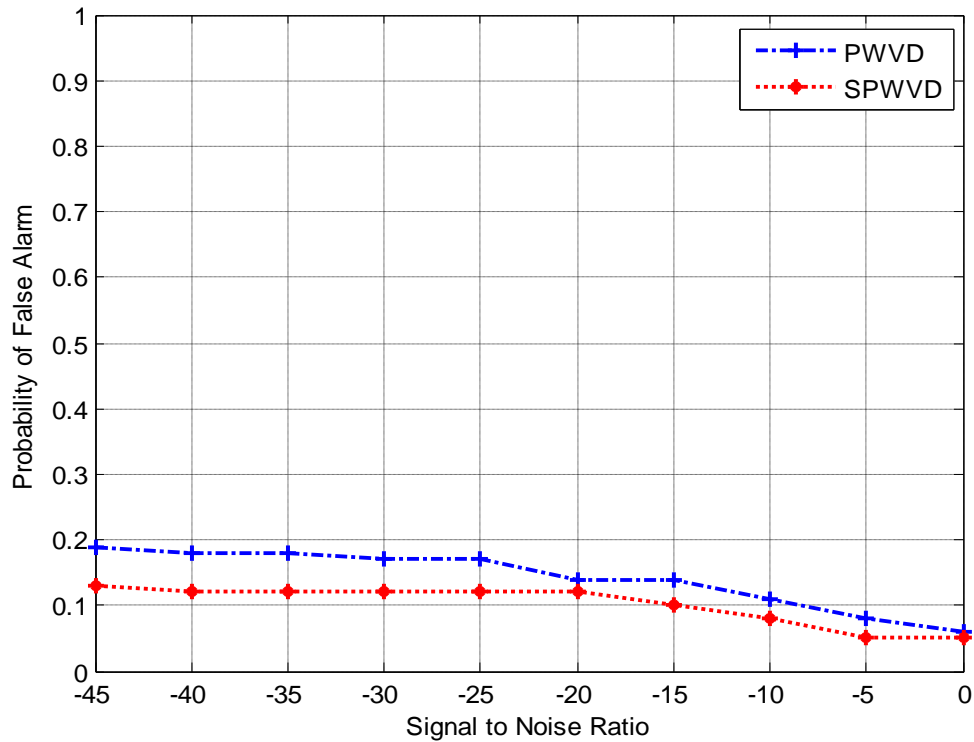


Figure 4.4 Plot of PFA against SNR for Rician channel condition

The PFA against SNR for Rician channel condition in Figure 4.4 shows performances the two techniques in terms of their probabilities of false alarm. The rician channel condition is a scenario of distortion in the communication channel with a dominant path from the three modeled paths. The PFA for SPWVD is lower with 4.1% reduction when compared to that of PWVD as recorded from the plots. This shows the improvement in the performance of SPWVD over PWVD.

Table 4.5 Data of SPWVD and PWVD with PMD for Rayleigh Channel Condition

SNR (dB)	SPWVD				PWVD			
	H_0	H_1	H_e	PMD	H_0	H_1	H_e	PMD
-45	08	74	18	0.24	22	59	19	0.32
-40	07	77	16	0.21	26	56	18	0.32
-35	08	76	16	0.21	21	61	18	0.30
-30	04	76	15	0.21	24	61	15	0.25
-25	05	83	12	0.15	27	59	14	0.24
-20	12	82	13	0.15	21	65	14	0.22
-15	05	82	04	0.15	28	60	12	0.20
-10	12	77	12	0.14	24	64	12	0.19
-5	04	85	11	0.13	26	63	11	0.18
0	11	79	10	0.13	19	71	10	0.14

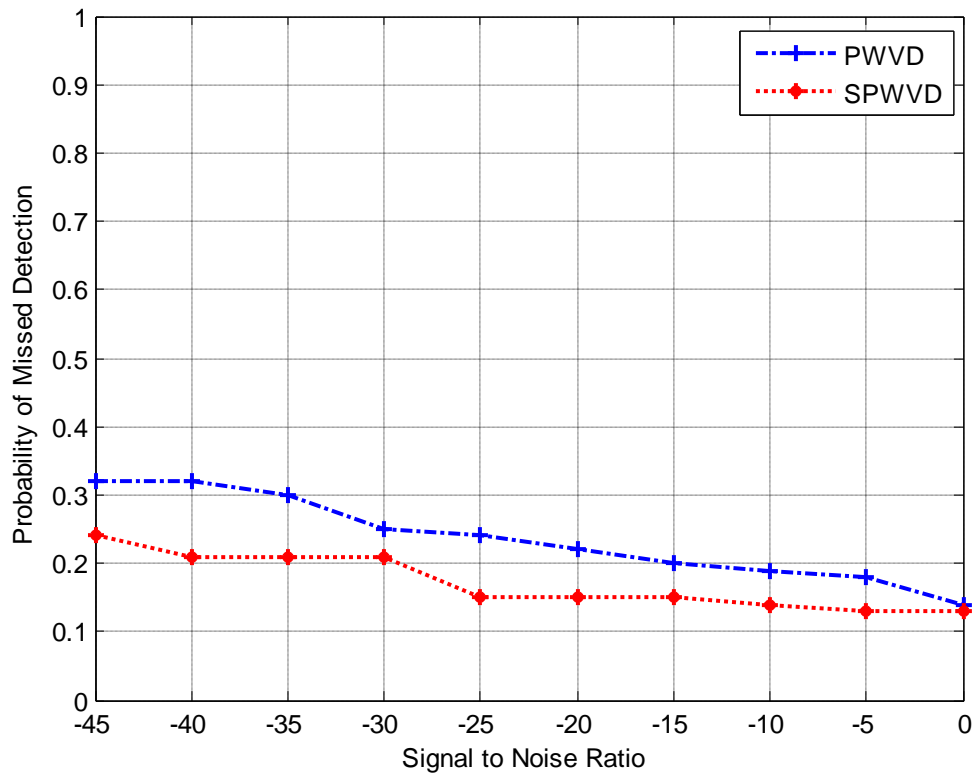


Figure 4.5 Plot of PMD against SNR for Rayleigh channel condition

In Figure 4.5, the PMD against SNR plots for SPWVD and PWVD are shown. The respective probabilities here under the Rayleigh channel condition are high. However, the performance of the SPWVD is better than that of PWVD as the probabilities of missed detection are lower by 6.4% reduction in the PMD on an average.

Table 4.6 Data SPWVD and PVWD with PFA for Rayleigh channel condition

SNR (dB)	SPWVD				PWVD			
	H_0	H_1	H_e	PFA	H_0	H_1	H_e	PFA
-45	81	09	10	0.12	63	21	16	0.25
-40	76	15	09	0.12	63	23	14	0.22
-35	80	12	08	0.10	71	16	13	0.18
-30	80	12	08	0.10	68	20	12	0.18
-25	77	15	08	0.10	62	27	11	0.18
-20	82	11	07	0.09	65	24	11	0.17
-15	81	12	07	0.09	65	24	11	0.17
-10	83	10	07	0.08	70	20	10	0.14
-5	87	08	05	0.06	73	18	09	0.12
0	82	13	05	0.06	79	12	09	0.11

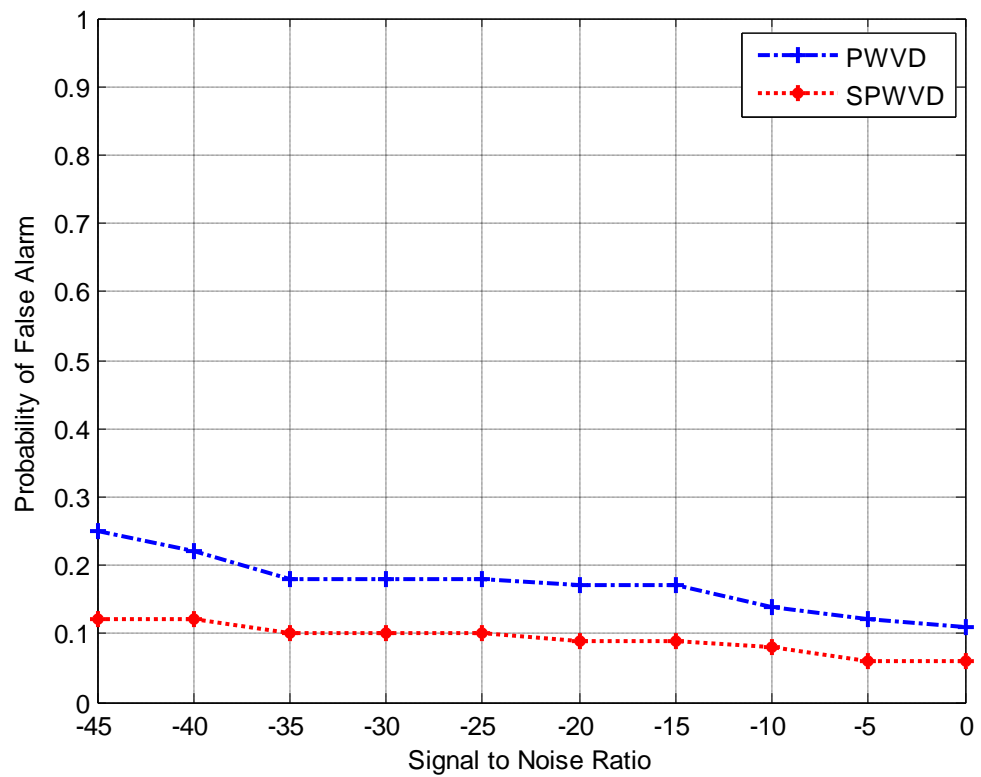


Figure 4.6 Plot of PFA against SNR for Rayleigh Channel Condition

From Figure 4.6, the probabilities of false alarm are plotted against SNR using the data in table 4.6. The probabilities of false alarm under Smoothed Pseudo Wigner-Ville Distribution (SPWVD) are lower than that of pseudo Wigner-Ville distribution (PWVD). The performance of the SPWVD is better as the PFAs that indicates how much falsely we can detect the primary user signal when it is not actually transmitting are not as high as that of PWVD, which shows 8% reduction in the PFA on an average for SPWVD over PWVD.

CHAPTER FIVE

CONCLUSION AND RECOMMENDATIONS

5.1 Summary

This work aimed at suppressing the effect of cross-term components that is inherent the use of time-frequency analysis for spectrum sensing. Smoothed Pseudo Wigner-Ville Distribution (SPWVD) was employed to suppress the cross-term effect with the intent of determining a better sensing threshold than the earlier time-frequency distribution techniques reportedly used in literature.

5.2 Conclusion

The smoothed pseudo Wigner-Ville distribution (SPWVD) technique has been utilized in this work to reduce the effect of cross-term components by way of employing two smoothing filters for filtering the cross-terms generated while seeking to analyze OFDMA user signal in both time and frequency domain simultaneously. SPWVD yields a better sensing threshold when compared with Pseudo Wigner-Ville Distribution (PWVD) distribution employed in the work of Monfared et al 2013. OFDMA user signal transmissions were simulated and analyzed in MATLAB R2013b environment and the time frequency toolbox that contains the time-frequency analysis techniques developed at CNRS were used to achieve the aim of this work. The determined threshold in the SPWVD technique was compared with that of PWVD for performance analysis and the SPWVD showed a superior performance in the respective channel conditions (AWGN, Rician and Rayleigh).

5.3 Significant contribution

Previous researches have applied the use of time-frequency analysis technique for spectrum sensing in cognitive in which Wigner-Ville distribution and pseudo Wigner-Ville distribution has been employed. The issue that existed in the earlier techniques is the cross-term component that affects the judgement of a good sensing threshold. This work has contributed to the research area by:

1. Applying smoothed pseudo Wigner-Ville distribution that utilized Kaiser-Bessel window and Blackman window to suppress the cross-term components and retain good resolution to estimate the energy spectral densities used in determining the sensing threshold.
2. The threshold estimated performed better in sensing with a 2.7% reduction in the missed detection probability and 3% reduction in the false alarm probability for AWGN, 4.7% and 4.7% reduction were recorded for Rician channel condition and 6.4% and 8% were also recorded for Rayleigh channel condition.

5.4 Recommendations

Possible areas in which this work can be extended to for further exploration in future researches are suggested below:

- (i) The optimal number of samples needed to be taken to for better spectrum sensing threshold determination can be investigated.
- (ii) The required sensing time as it relates to the sensing threshold for better performance can also be researched into.

- (iii) The SPWVD of the time-frequency analysis techniques can be employed in a cooperative manner in which two or more secondary users run the same algorithm in a particular geolocation on the same primary user band for better spectrum holes opportunities.

REFERENCES

- Aguilar-Gonzalez, R., Cardenas-Juarez, M., Rico, U. P., & Stevens-Navarro, E. (2013). Power Spectrum Measurements from 30 MHz to 910 MHz in the City of San Luis Potosi, Mexico. *Procedia Technology*, 7, 30-36.
- Angrisani, L., Betta, G., Capriglione, D., Cerro, G., Ferrigno, L., & Miele, G. (2014). *Proposal and analysis of new algorithms for wideband spectrum sensing in cognitive radio*. Paper presented at the 2014 IEEE International Instrumentation and Measurement Technology Conference (I2MTC) Proceedings.
- Arthy, A., & Periyasamy, P. (2015). *A Review on Spectrum Sensing Techniques in Cognitive Radio Network*. Paper presented at the Proceedings of the UGC Sponsored National Conference on Advanced Networking and Applications.
- Atapattu, S., Tellambura, C., & Jiang, H. (2014). *Energy detection for spectrum sensing in cognitive radio*: Springer.
- Auger, F., Flandrin, P., Goncalves, P., & Lemoine, O. (2005). *Time-Frequency Toolbox for use with MATLAB*. Retrieved from <http://tftb.nongnu.org/>
- Awon, N. T., Islam, M., Rahman, M., & Islam, A. (2012). Effect of AWGN & Fading (Rayleigh & Rician) channels on BER performance of a WiMAX communication System. *arXiv preprint arXiv:1211.4294*.
- Ayeni, A. A., Faruk, N., Bello, O. W., Sowande, O. A., Onidare, S. O., & Muhammad, M. Y. (2016). Spectrum Occupancy Measurements and Analysis in the 2.4-2.7 GHz Band in Urban and Rural Environments. *International Journal of Future Computer and Communication*, 5(3), 142.
- Babalola, O., Garba, E., Oladimeji, I., Bamiduro, A., Faruk, N., Sowande, O., Muhammad, M. (2015). *Spectrum occupancy measurements in the TV and CDMA bands*. Paper presented at the 2015 International Conference on Cyberspace (CYBER-Abuja).
- Bektas, C., Akan, A., & Odabasioglu, N. (2012). *Energy based spectrum sensing using wavelet transform for fading channels*. Paper presented at the 2012 4th International Congress on Ultra Modern Telecommunications and Control Systems and Workshops (ICUMT)

- Berbra, K., Barkat, M., Gini, F., Greco, M., & Stinco, P. (2016). A fast spectrum sensing for CP-OFDM cognitive radio based on adaptive thresholding. *Signal Processing*, 128, 252-261.
- Biagi, M., Rinauro, S., Colonnese, S., Scarano, G., & Cusani, R. (2014). WiVCoRA: Wigner–Ville Cognitive Radio Access for Secondary Nodes. *Vehicular Technology, IEEE Transactions on*, 63(9), 4248-4264.
- Biglieri, E., Goldsmith, A. J., Greenstein, L. J., Mandayam, N. B., & Poor, H. V. (2012). *Principles of cognitive radio*: Cambridge University Press.
- Boashash, B. (2015). *Time-frequency signal analysis and processing: a comprehensive reference*: Academic Press.
- Brooker, G. (2008). *Introduction to Sensors for Ranging and Imaging*. USA: SciTechPublishing Inc.
- Christodoulou, C., & Jayaweera, S. (2011). Radiobots: Architecture, Algorithms and Realtime Reconfigurable Antenna Designs for Autonomous, Self-learning Future Cognitive Radios.
- Dikmese, S. (2015). Enhanced Spectrum Sensing Techniques for Cognitive Radio Systems. *Tampereen teknillinen yliopisto. Julkaisu-Tampere University of Technology. Publication; 1280*.
- Dikmese, S., Renfors, M., & Dincer, H. (2011). *FFT and filter bank based spectrum sensing for WLAN signals*. Paper presented at the 2011 20th European Conference on Circuit Theory and Design (ECCTD)
- Gardner, W. A. (1991). Exploitation of spectral redundancy in cyclostationary signals. *Signal Processing Magazine, IEEE*, 8(2), 14-36.
- Guibene, W., Turki, M., Zayen, B., & Hayar, A. (2012). Spectrum sensing for cognitive radio exploiting spectrum discontinuities detection. *EURASIP Journal on Wireless Communications and Networking*, 2012(1), 1-9.
- Hamid, M., Bjorsell, N., Van Moer, W., Barbe, K., & Slimane, S. B. (2013). Blind spectrum sensing for cognitive radios using discriminant analysis: A novel approach. *IEEE Transactions on Instrumentation and Measurement*, 62(11), 2912-2921.
- Hiremath, S., Patra, S., & Mishra, A. (2015). Spectrum Sensing for Cognitive Radio using S-method based Joint Time-Frequency Representation.
- Ian Poole (2016). *IEEE 802.22 Spectrum Sensing and Cognitive Network*. Retrieved from <http://www.radio-electronics.com/info/wireless/ieee-802-22/cognitive-network-spectrum-sensing.php>

- IEEE 802.22a-2014. (2014). IEEE Recommended Practice for Information Technology – Telecommunications and information exchange between systems Wireless Regional Area Networks (WRAN) - Specific requirements - Part 22: Cognitive Wireless RAN Medium Access Control (MAC) and Physical Layer (PHY) Specifications: Policies and Procedures for Operation in the TV Bands, Amendment 1: Management and Control Plane Interfaces and Procedures and Enhancement to the Management Information Base (MIB)
- IEEE 802.22.2-2012. (2012). IEEE Recommended Practice for Information Technology – Telecommunications and information exchange between systems Wireless Regional Area Networks (WRAN) - Specific requirements – Part 22.2: Installation and Deployment of IEEE 802.22 Systems.
- Ingram, D. M. A., Acosta, G., & Matlab, O. S. U. (2000). Smart Antenna Research Laboratory. *Guillermo Acosta August*.
- Javed, F., & Mahmood, A. (2010). *The use of time frequency analysis for spectrum sensing in cognitive radios*. Paper presented at the 2010 4th International Conference on Signal Processing and Communication Systems (ICSPCS)
- Javed, F., Shafi, I., & Mahmood, A. (2012). A novel radio mode identification approach for spectrum sensing in cognitive radios. *International Journal of Communication Networks and Information Security*, 4(2), 86.
- Jouini, W. (2011). Energy detection limits under log-normal approximated noise uncertainty. *Signal Processing Letters, IEEE*, 18(7), 423-426.
- Kolodzy, P., & Avoidance, I. (2002). Spectrum policy task force. *Federal Commun. Comm., Washington, DC, Rep. ET Docket(02-135)*.
- Kumar, S., Gupta, P., Singh, G., & Chauhan, D. (2013). Performance analysis of Rayleigh and Rician fading channel models using Matlab simulation. *International Journal of Intelligent Systems and Applications*, 5(9), 94.
- Lopez-Benitez, M., & Casadevall, F. (2013). Signal uncertainty in spectrum sensing for cognitive radio. *IEEE Transactions on Communications*, 61(4), 1231-1241.
- McHenry, M., & McCloskey, D. (2004). New York City spectrum occupancy measurements september 2004. *Shared Spectrum Company, www.sharedspectrum.com*.
- Monfared, S. S., Taherpour, A., & Khattab, T. (2013). *Time-frequency compressed spectrum sensing in cognitive radios*. Paper presented at the Global Communications Conference (GLOBECOM), 2013 IEEE.
- Mounika, B., Chandra, K. R., & Kumar, R. R. (2013). Spectrum sensing techniques and issues in cognitive radio. *International Journal of Engineering Trends and Technology (IJETT)-ISSN, 2231-5381*.

- National Instruments. (2016). Other Cohen's Class Time Frequency Distributions (Advanced Signal Processing Toolkit). from https://zone.ni.com/reference/en-XX/help/371419D-01/lvasptconcepts/tfa_cwd_csd/
- Paul, P., Xin, C., Song, M., & Zhao, Y. (2015). *Spectrum Sensing for a Subdivided Band in Cognitive Radio Networks*. Paper presented at the 2015 24th International Conference on Computer Communication and Networks (ICCCN).
- Smith, J.O. Mathematics of the Discrete Fourier Transform (DFT) with Audio Applications, Second Edition, <http://ccrma.stanford.edu/~jos/mdft/>, online book, 2007 edition, accessed 15 October 2016.
- Subheddar, M., & Birajdar, G. (2011). Spectrum sensing techniques in cognitive radio networks: a survey. *International Journal of Next-Generation Networks*, 3(2), 37-51.
- Tandra, R., & Sahai, A. (2008a). *Noise calibration, delay coherence and SNR walls for signal detection*. Paper presented at the 3rd IEEE Symposium on New Frontiers in Dynamic Spectrum Access Networks, 2008. DySPAN 2008.
- Tandra, R., & Sahai, A. (2008b). SNR walls for signal detection. *Selected Topics in Signal Processing, IEEE Journal of*, 2(1), 4-17.
- Tawk, Y., Costantine, J., & Christodoulou, C. G. (2014). Cognitive-radio and antenna functionalities: A tutorial [Wireless Corner]. *Antennas and Propagation Magazine, IEEE*, 56(1), 231-243.
- Vaidehi, G., Swetha, N., & Sastry, P. N. (2015). Entropy based Spectrum Sensing in Cognitive Radio Networks. *Entropy*, 4(11).
- Viswanathan, M. (2013). Simulation of digital communication systems using Matlab. *Mathuranathan Viswanathan at Smashwords*.
- Weiss, M. B., Lehr, W., Altamimi, M., & Cui, L. (2012). "Enforcement in dynamic spectrum access systems" in TPRC, Telecommunications Policy, vol. 36, no. 4, pp. 335-348.

APPENDIX A

OFDM SIMULATION mFILE CODE

```
function time_wave_rx = OFDM_SIM(n)

% ##### %
% ***** OFDM SYSTEM INITIALIZATION: ***** %
% **** setting up parameters & obtaining source data **** %
% ##### %
% Turn off exact-match warning to allow case-insensitive input files
warning('off', 'MATLAB:dispatcher:InexactMatch');
% clear all; % clear all previous data in MATLAB workspace
% close all; % close all previously opened figures and graphs
fprintf('\n\n#####\n')
fprintf('#***** OFDM Simulation *****#\n')
fprintf('#####\n\n')

% invoking ofdm_parameters.m script to set OFDM system parameters
% ofdm_parameters;
% ***** PARAMETERS INITIALIZATION ***** %
% This file configures parameters for the OFDM system.
% input/output file names
file_in = [];
while isempty(file_in)
file_in = 'tafnew.bmp'; %input('source data filename: ', 's');
if exist([pwd '/' file_in], 'file')~=2
fprintf ...
('%s" does not exist in current directory.\n', file_in);
file_in = [];
end
end
file_out = [file_in(1:length(file_in)-4) '_OFDM.bmp'];
disp(['Output file will be: ' file_out])
% size of Inverse Fast Fourier Transform (must be power of 2)
ifft_size = 0.1; % force into the while loop below
while (isempty(ifft_size) || ...
(rem(log2(ifft_size),1) ~= 0 || ifft_size < 8))
ifft_size = 2048; %input('IFFT size: ');
if (isempty(ifft_size) || ...
(rem(log2(ifft_size),1) ~= 0 || ifft_size < 8))
disp('IFFT size must be at least 8 and power of 2.')
end
end
end
```

```

% number of carriers
carrier_count = ifft_size; % force into the while loop below
while (isempty(carrier_count) || ...
(carrier_count>(ifft_size/2-2)) || carrier_count<2)
carrier_count = 1009; %input('Number of carriers: ');
if (isempty(carrier_count) || (carrier_count > (ifft_size/2-2)))
disp('Must NOT be greater than ("IFFT size"/2-2)')
end
end
% bits per symbol (1 = BPSK, 2=QPSK, 4=16PSK, 8=256PSK)
symb_size = 0; % force into the while loop below
while (isempty(symb_size) || ...
(symb_size~=1 && symb_size~=2 && symb_size~=4 && symb_size~=8))
symb_size = 4; %input('Modulation(1=BPSK, 2=QPSK, 4=16PSK, 8=256PSK): ');
if (isempty(symb_size) || ...
(symb_size~=1&&symb_size~=2&&symb_size~=4&&symb_size~=8))
disp('Only 1, 2, 4, or 8 can be choosen')
end
end
% channel clipping in dB
clipping = [];
while isempty(clipping)
clipping = 9; %input('Amplitude clipping introduced by communication
channel (in dB):');
end

% signal to noise ratio in dB
SNR_dB = [];
while isempty(SNR_dB)
SNR_dB = n; %input('Signal-to-Noise Ratio (SNR) in dB: ');
end

word_size = 8; % bits per word of source data (byte)
guard_time = ifft_size/4; % length of guard interval for each symbol period
% 25% of ifft_size
% number of symbols per carrier in each frame for transmission
symb_per_frame = ceil(2^13/carrier_count);
% === Derived Parameters === %
% frame_len: length of one symbol period including guard time
symb_period = ifft_size + guard_time;
% head_len: length of the header and trailer of the transmitted data
head_len = symb_period*8;
% envelope: symb_period/envelope is the size of envelope detector
envelope = ceil(symb_period/256)+1;
% === carriers assigned to IFFT bins === %
% spacing for carriers distributed in IFFT bins
spacing = 0;
while (carrier_count*spacing) <= (ifft_size/2 - 2)
spacing = spacing + 1;
end
spacing = spacing - 1;
% spread out carriers into IFFT bins accordingly
midFreq = ifft_size/4;
first_carrier = midFreq - round((carrier_count-1)*spacing/2);
last_carrier = midFreq + floor((carrier_count-1)*spacing/2);
carriers = [first_carrier:spacing:last_carrier] + 1;

```

```

conj_carriers = ifft_size - carriers + 2;

% save parameters for receiver
save('ofdm_parameters');
x = imread(file_in);
% arrange data read from image for OFDM processing
h = size(x,1);
w = size(x,2);
x = reshape(x', 1, w*h);
baseband_tx = double(x);
% convert original data word size (bits/word) to symbol size (bits/symbol)
% symbol size (bits/symbol) is determined by choice of modulation method
baseband_tx = ofdm_base_convert(baseband_tx, word_size, symb_size);
% save original baseband data for error calculation later
save('err_calc.mat', 'baseband_tx');
% ##### %
% ***** OFDM TRANSMITTER ***** %
% ##### %
tic; % start stopwatch
% generate header and trailer (an exact copy of the header)
f = 0.25;
header = sin(0:f*2*pi:f*2*pi*(head_len-1));
f=f/(pi*2/3);
header = header+sin(0:f*2*pi:f*2*pi*(head_len-1));
% arrange data into frames and transmit
frame_guard = zeros(1, symb_period);
time_wave_tx = [];
symb_per_carrier = ceil(length(baseband_tx)/carrier_count);
fig = 1;
if (symb_per_carrier > symb_per_frame) % === multiple frames === %
power = 0;
while ~isempty(baseband_tx)
% number of symbols per frame
frame_len = min(symb_per_frame*carrier_count,length(baseband_tx));
frame_data = baseband_tx(1:frame_len);
% update the yet-to-modulate data
baseband_tx = baseband_tx((frame_len+1):(length(baseband_tx)));
% OFDM modulation
time_signal_tx = ofdm_modulate(frame_data,ifft_size,carriers,...
conj_carriers, carrier_count, symb_size, guard_time, fig);
fig = 0; %indicate that ofdm_modulate() has already generated plots
% add a frame guard to each frame of modulated signal
time_wave_tx = [time_wave_tx frame_guard time_signal_tx];
frame_power = var(time_signal_tx);
end
% scale the header to match signal level
power = power + frame_power;
% The OFDM modulated signal for transmission
time_wave_tx = [power*header time_wave_tx frame_guard power*header];
else% === single frame === %
% OFDM modulation
time_signal_tx = ofdm_modulate(baseband_tx,ifft_size,carriers,...
conj_carriers, carrier_count, symb_size, guard_time, fig);
% calculate the signal power to scale the header
power = var(time_signal_tx);
% The OFDM modulated signal for transmission
time_wave_tx = ...

```

```

[power*header frame_guard time_signal_tx frame_guard power*header];
end
% show summary of the OFDM transmission modeling
peak = max(abs(time_wave_tx(head_len+1:length(time_wave_tx)-head_len)));
sig_rms = std(time_wave_tx(head_len+1:length(time_wave_tx)-head_len));
peak_rms_ratio = (20*log10(peak/sig_rms));
fprintf('\nSummary of the OFDM transmission and channel modeling:\n')
fprintf('Peak to RMS power ratio at entrance of channel is: %f dB\n', ...
peak_rms_ratio)
% ##### %
% ***** COMMUNICATION CHANNEL ***** %
% ##### %
% ===== signal clipping ===== %
clipped_peak = (10^(0-(clipping/20)))*max(abs(time_wave_tx));
time_wave_tx(find(abs(time_wave_tx)>=clipped_peak))...
= clipped_peak.*time_wave_tx(find(abs(time_wave_tx)>=clipped_peak))...
./abs(time_wave_tx(find(abs(time_wave_tx)>=clipped_peak)));

% % ===== channel noise ===== %
% % power = var(time_wave_tx); % Gaussian (AWGN)
% % SNR_linear = 10^(SNR_dB/10);
% % noise_factor = sqrt(power/SNR_linear);
% % noise = randn(1,length(time_wave_tx)) * noise_factor;
% % time_wave_rx = time_wave_tx + noise;
% % size(time_wave_tx)

% % AWGN channel
% size(time_wave_tx)
% Tx_Packet=time_wave_tx(1,1:65536);
% y = awgn(Tx_Packet, SNR_dB, 'measured');
% time_wave_rx = y;
% % y.StoreHistory = true;
% % Rx_Packet = filter(y, Tx_Packet);
% % Rx_Packet;

% show summary of the OFDM channel modeling
peak = max(abs(time_wave_rx(head_len+1:length(time_wave_rx)-head_len)));
sig_rms = std(time_wave_rx(head_len+1:length(time_wave_rx)-head_len));
peak_rms_ratio = (20*log10(peak/sig_rms));
fprintf('Peak to RMS power ratio at exit of channel is: %f dB\n', ...
peak_rms_ratio)
% Save the signal to be received
save ('transmitted.mat', 'time_wave_rx');
save('received.mat', 'time_wave_rx', 'h', 'w');
fprintf('#***** OFDM data transmitted in %f seconds *****#\n\n', toc)
fprintf('#####\n\n')

```

APPENDIX B

RAYLEIGH CHANNEL mFILE CODE

```
%rayleigh noise
size(time_wave_tx)
Tx_Packet=time_wave_tx(1,1:65536);
Ts=1e-4; %1e-4; % sampling time in second
Fd=100; % doppler frequency in Hz
Tau=[0 1.5e-4 2.5e-4]; % delay for the three paths
PdB=[-2, -2, -6]; % power in each of the three paths
pkt_allones=ones(1,480)+i*ones(1,480);
% Rayleigh channel model
h = rayleighchan(Ts, Fd, Tau, PdB);
h.StoreHistory = true;
Rx_pkt_allones = filter(h, pkt_allones);
Rx_Packet = filter(h, Tx_Packet); % passing baseband IQ vector through
rayleigh channel
time_wave_rx = Rx_Packet;
```

APPENDIX C

RICIAN CHANNEL mFILE CODE

```
% %Rician Channel
size(time_wave_tx)
Tx_Packet=time_wave_tx(1,1:65536);
KFactor = 3; % Rician K-factor
Ts=1e-4; % sampling time in second
Fd=100; % doppler frequency in Hz
Tau=[0 1.5e-4 2.5e-4]; % delay for the three paths
PdB=[0, -2, -6]; % power in each of the three paths
pkt_allones=ones(1,480)+i*ones(1,480);
% % rician channel model
h = ricianchan(Ts, Fd, KFactor, Tau, PdB);
h.StoreHistory = true;
Rx_pkt_allones = filter(h, pkt_allones);
Rx_Packet = filter(h, Tx_Packet); % passing baseband IQ vector through rician
channel
% time_wave_rx = Rx_Packet;
```

APPENDIX D

OFDM PARAMETERS mFILE CODE

```
% ***** PARAMETERS INITIALIZATION ***** %
% This file configures parameters for the OFDM system.
% input/output file names
file_in = [];
while isempty(file_in)
file_in = input('source data filename: ', 's');
if exist([pwd '/' file_in], 'file')~=2
fprintf ...
('%s" does not exist in current directory.\n', file_in);
file_in = [];
end
end
file_out = [file_in(1:length(file_in)-4) '_OFDM.bmp'];
disp(['Output file will be: ' file_out])
% size of Inverse Fast Fourier Transform (must be power of 2)
ifft_size = 0.1; % force into the while loop below
while (isempty(ifft_size) || ...
(rem(log2(ifft_size),1) ~= 0 || ifft_size < 8))
ifft_size = input('IFFT size: ');
if (isempty(ifft_size) || ...
(rem(log2(ifft_size),1) ~= 0 || ifft_size < 8))
disp('IFFT size must be at least 8 and power of 2.')
end
end
% number of carriers
carrier_count = ifft_size; % force into the while loop below
while (isempty(carrier_count) || ...
(carrier_count > (ifft_size/2-2) || carrier_count < 2))
carrier_count = input('Number of carriers: ');
if (isempty(carrier_count) || (carrier_count > (ifft_size/2-2)))
disp('Must NOT be greater than ("IFFT size"/2-2)')
end
end
% bits per symbol (1 = BPSK, 2=QPSK, 4=16PSK, 8=256PSK)
symb_size = 0; % force into the while loop below
while (isempty(symb_size) || ...
(symb_size~=1 && symb_size~=2 && symb_size~=4 && symb_size~=8))
symb_size = input...
('Modulation(1=BPSK, 2=QPSK, 4=16PSK, 8=256PSK): ');
if (isempty(symb_size) || ...
(symb_size~=1&&symb_size~=2&&symb_size~=4&&symb_size~=8))
disp('Only 1, 2, 4, or 8 can be choosen')
end
end
end
```

```

% channel clipping in dB
clipping = [];
while isempty(clipping)
clipping = input...
('Amplitude clipping introduced by communication channel (in dB):');
end
% signal to noise ratio in dB
SNR_dB = [];
while isempty(SNR_dB)
SNR_dB = input('Signal-to-Noise Ratio (SNR) in dB: ');
end
word_size = 8; % bits per word of source data (byte)
guard_time = ifft_size/4; % length of guard interval for each symbol period
% 25% of ifft_size
% number of symbols per carrier in each frame for transmission
symb_per_frame = ceil(2^13/carrier_count);
% === Derived Parameters === %
% frame_len: length of one symbol period including guard time
symb_period = ifft_size + guard_time;
% head_len: length of the header and trailer of the transmitted data
head_len = symb_period*8;
% envelope: symb_period/envelope is the size of envelope detector
envelope = ceil(symb_period/256)+1;
% === carriers assigned to IFFT bins === %
% spacing for carriers distributed in IFFT bins
spacing = 0;
while (carrier_count*spacing) <= (ifft_size/2 - 2)
spacing = spacing + 1;
end
spacing = spacing - 1;
% spread out carriers into IFFT bins accordingly
midFreq = ifft_size/4;
first_carrier = midFreq - round((carrier_count-1)*spacing/2);
last_carrier = midFreq + floor((carrier_count-1)*spacing/2);
carriers = [first_carrier:spacing:last_carrier] + 1;
conj_carriers = ifft_size - carriers + 2;

```

APPENDIX E

OFDM BASE CONVERSION mFILE CODE

```
% ***** FUNCTION: ofdm_base_convert() ***** %
% This function converts data from one base to another.
% "Base" refers to number of bits the symbol/word uses to represent data.
function data_out = ofdm_base_convert(data_in, base, new_base)
% if new base is in a higher order than the current base,
% make the size of data in current base a multiple of its new base
if new_base > base
data_in = data_in(1:...
floor(length(data_in)/(new_base/base))*(new_base/base));
end
% base to binary
for k=1:base
binary_matrix(k,:) = floor(data_in/2^(base-k));
data_in = rem(data_in,2^(base-k));
end
% format the binary matrix to fit dimensions of the new base
newbase_matrix = reshape(binary_matrix, new_base, ...
size(binary_matrix,1)*size(binary_matrix,2)/new_base);
% binary to new_base
data_out = zeros(1, size(newbase_matrix,2));
for k=1:new_base
data_out = data_out + newbase_matrix(k,:)*(2^(new_base-k));
end
```

APPENDIX F

OFDM MODULATION mFILE CODE

```
% ***** FUNCTION: ofdm_modulation() ***** %
% This function performance the OFDM modulation before data transmission.
function signal_tx = ofdm_modulate(data_tx, ifft_size, carriers, ...
conj_carriers, carrier_count, symb_size, guard_time, fig)
% symbols per carrier for this frame
carrier_symb_count = ceil(length(data_tx)/carrier_count);
% append zeros to data with a length not multiple of number of carriers
if length(data_tx)/carrier_count ~= carrier_symb_count,
padding = zeros(1, carrier_symb_count*carrier_count);
padding(1:length(data_tx)) = data_tx;
data_tx = padding;
end
% serial to parellel: each column represents a carrier
data_tx_matrix = reshape(data_tx, carrier_count, carrier_symb_count)';
% ----- %
% ##### Differential Encoding ##### %
% ----- %
% an additional row and include reference point
carrier_symb_count = size(data_tx_matrix,1) + 1;
diff_ref = round(rand(1, carrier_count)*(2^symb_size)+0.5);
data_tx_matrix = [diff_ref; data_tx_matrix];
for k=2:size(data_tx_matrix,1)
data_tx_matrix(k,:) = ...
rem(data_tx_matrix(k, :)+data_tx_matrix(k-1, :), 2^symb_size);
end
% ----- %
% ## PSK (Phase Shift Keying) modulation ### %
% ----- %
% convert data to complex numbers:
% Amplitudes: 1; Phaes: converted from data using constellation mapping
[X,Y] = pol2cart(data_tx_matrix*(2*pi/(2^symb_size)), ...
ones(size(data_tx_matrix)));
complex_matrix = X + i*Y;
% ----- %
% ##### assign IFFT bins to carriers and imaged carriers ##### %
% ----- %
spectrum_tx = zeros(carrier_symb_count, ifft_size);
spectrum_tx(:,carriers) = complex_matrix;
spectrum_tx(:,conj_carriers) = conj(complex_matrix);
% Figure(1) and Figure(2) can both shhow OFDM Carriers on IFFT bins
if fig==1
figure(1)
stem(1:ifft_size, abs(spectrum_tx(2, :)), 'b*-')
grid on
axis ([0 ifft_size -0.5 1.5])
ylabel('Magnitude of PSK Data')
```

```

xlabel('IFFT Bin')
title('OFDM Carriers on designated IFFT bins')
figure(2)
plot(1:ifft_size, (180/pi)*angle(spectrum_tx(2,1:ifft_size)), 'go')
hold on
grid on
stem(carriers, (180/pi)*angle(spectrum_tx(2,carriers)), 'b*-')
stem(conj_carriers, ...
(180/pi)*angle(spectrum_tx(2,conj_carriers)), 'b*-')
axis ([0 ifft_size -200 +200])
ylabel('Phase (degree)')
xlabel('IFFT Bin')
title('Phases of the OFDM modulated Data')
end
% ----- %
% ##### obtain time wave from spectrums waveform using IFFT ##### %
% ----- %
signal_tx = real(ifft(spectrum_tx'))';
% imag_signal_tx= imag(ifft(spectrum_tx'))';
% plot one symbol period of the time signal to be transmitted
if fig==1
% OFDM Time Signal (1 symbol period in one carrier)
limt = 1.1*max(abs(reshape(signal_tx',1,size(signal_tx,1)...
*size(signal_tx,2))));
figure (3)
plot(1:ifft_size, signal_tx(2,:))
grid on
axis ([0 ifft_size -limt limt])
ylabel('Amplitude')
xlabel('Time')
title('OFDM Time Signal (one symbol period in one carrier)')
% OFDM Time Signal (1 symbol period in a few samples of carriers)
figure(4)
colors = ['b','g','r','c','m','y'];
realSig=[];
% imagSig=[];
for k=1:min(length(colors),(carrier_symb_count-1))
plot(1:ifft_size, signal_tx(k+1,:))
plot(1:ifft_size, signal_tx(k+1,:), colors(k))
realSig=[realSig, signal_tx(k+1,:)];
% imagSig=[imagSig, imag_signal_tx(k+1,:)];
hold on
end
save('realSig.mat', 'realSig');
% save('imagSig.mat', 'imagSig');
grid on
axis ([0 ifft_size -limt limt])
ylabel('Amplitude')
xlabel('Time')
title('Samples of OFDM Time Signals over one symbol period')
end
sig = (load('realSig.mat'));
signal_tx = sig.realSig;
% ----- %
% ##### add a periodic guard time ##### %
% ----- %
end_symb = size(signal_tx, 2); % end of a symbol period without guard

```

```

signal_tx = [signal_tx(:,(end_symb-guard_time+1):end_symb) signal_tx];
% parellel to serial
signal_tx = signal_tx'; % MATLAB's reshape goes along with columns
signal_tx = reshape(signal_tx, 1, size(signal_tx,1)*size(signal_tx,2));

```

APPENDIX G

SPWVD mFILE CODE

```

function [tfr,t,f] = tfrspwv(x,t,N,g,h,trace);
%TFRSPWV Smoothed Pseudo Wigner-Ville time-frequency distribution.
% [TFR,T,F]=TFRSPWV(X,T,N,G,H,TRACE) computes the Smoothed Pseudo
% Wigner-Ville distribution of a discrete-time signal X, or the
% cross Smoothed Pseudo Wigner-Ville representation between two
% signals.
%
% X      : signal if auto-SPWV, or [X1,X2] if cross-SPWV.
% T      : time instant(s)          (default : 1:length(X))
% N      : number of frequency bins (default : length(X)).
% G      : time smoothing window, G(0) being forced to 1.
%                (default : Hamming(N/10)).
% H      : frequency smoothing window in the time-domain,
% H(0) being forced to 1 (default : Hamming(N/4)).
% TRACE  : if nonzero, the progression of the algorithm is shown
%                (default : 0).
% TFR    : time-frequency representation. When called without
% output arguments, TFRSPWV runs TFRQVIEW.
% F      : vector of normalized frequencies.
%
% Example :
% sig=fmlin(128,0.05,0.15)+fmlin(128,0.3,0.4);
% g=tftb_window(15,'Kaiser'); h=tftb_window(63,'Kaiser');
% [tfr,t,f] = tfrspwv(sig,1:128,64,g,h,1);
%
if (nargin == 0),
    error('At least 1 parameter required');
end;
[xrow,xcol] = size(x);
if (xcol==0)|(xcol>2),
    error('X must have one or two columns');
end

if (nargin <= 2),
    N=xrow;
elseif (N<0),
    error('N must be greater than zero');
elseif (2^nextpow2(N)~=N),
    fprintf('For a faster computation, N should be a power of two\n');
end;

hlength=floor(N/4); hlength=hlength+1-rem(hlength,2);
glength=floor(N/10);glength=glength+1-rem(glength,2);

```

```

if (nargin == 1),
    t=1:xrow; g = tftb_window(glenght); h = tftb_window(hlenght); trace = 0;
elseif (nargin == 2)|(nargin == 3),
    g = tftb_window(glenght); h = tftb_window(hlenght); trace = 0;
elseif (nargin == 4),
    h = tftb_window(hlenght); trace = 0;
elseif (nargin == 5),
    trace = 0;
end;

[trow,tcol] = size(t);
if (trow~=1),
    error('T must only have one row');
end;

[grow,gcol]=size(g); Lg=(grow-1)/2; % g=g/sum(g);
if (gcol~=1)|(rem(grow,2)==0),
    error('G must be a smoothing window with odd length');
end;

[hrow,hcol]=size(h); Lh=(hrow-1)/2; h=h/h(Lh+1);
if (hcol~=1)|(rem(hrow,2)==0),
    error('H must be a smoothing window with odd length');
end;

tfr= zeros (N,tcol) ;
if trace, disp('Smoothed pseudo Wigner-Ville distribution'); end;
for icol=1:tcol,
    ti= t(icol); taumax=min([ti+Lg-1,xrow-ti+Lg,round(N/2)-1,Lh]);
if trace, disp('tau='); end;
points= -min([Lg,xrow-ti]):min([Lg,ti-1]);
g2=g(Lg+1+points); g2=g2/sum(g2);
tfr(1,icol)= sum(g2 .* x(ti-points,1) .* conj(x(ti-points,xcol)));
for tau=1:taumax,
    points= -min([Lg,xrow-ti-tau]):min([Lg,ti-tau-1]);
    g2=g(Lg+1+points); g2=g2/sum(g2);
    R=sum(g2 .* x(ti+tau-points,1) .* conj(x(ti-tau-points,xcol)));
    tfr( 1+tau,icol)=h(Lh+tau+1)*R;
    R=sum(g2 .* x(ti-tau-points,1) .* conj(x(ti+tau-points,xcol)));
    tfr(N+1-tau,icol)=h(Lh-tau+1)*R;
end;
tau=round(N/2);
if (ti<=xrow-tau)&(ti>=tau+1)&(tau<=Lh),
    points= -min([Lg,xrow-ti-tau]):min([Lg,ti-tau-1]);
    g2=g(Lg+1+points); g2=g2/sum(g2);
    tfr(tau+1,icol) = 0.5 * ...
        (h(Lh+tau+1)*sum(g2 .* x(ti+tau-points,1) .* conj(x(ti-tau-
points,xcol)))+...
        h(Lh-tau+1)*sum(g2 .* x(ti-tau-points,1) .* conj(x(ti+tau-
points,xcol))));
end;
end;
if trace, fprintf('\n'); end;
tfr= fft(tfr);
if (xcol==1), tfr=real(tfr); end ;

```

```

if (nargout==0),
    tfrqview(tfr,x,t,'tfrspwv',g,h);
elseif (nargout==3),
    f=(0.5*(0:N-1)/N)';
end;

```

APPENDIX H

PWVD mFILE CODE

```

function [tfr,t,f] = tfrpwv(x,t,N,h,trace);
%TFRPWV Pseudo Wigner-Ville time-frequency distribution.
% [TFR,T,F]=TFRPWV(X,T,N,H,TRACE) computes the Pseudo Wigner-Ville
% distribution of a discrete-time signal X, or the
% cross Pseudo Wigner-Ville representation between two signals.
%
% X      : signal if auto-PWV, or [X1,X2] if cross-PWV.
% T      : time instant(s)          (default : 1:length(X)).
% N      : number of frequency bins (default : length(X)).
% H      : frequency smoothing window, in the time-domain,
%          H(0) being forced to 1   (default : Hamming(N/4)).
% TRACE  : if nonzero, the progression of the algorithm is shown
%          (default : 0).
% TFR    : time-frequency representation. When called without
%          output arguments, TFRPWV runs TFRQVIEW.
% F      : vector of normalized frequencies.
%
% Example:
% sig=fmlin(128,0.1,0.4); tfrpwv(sig);
%
[xrow,xcol] = size(x);
if (nargin < 1),
    error('At least 1 parameter is required');
elseif (nargin <= 2),
    N=xrow;
end;

hlength=floor(N/4);
hlength=hlength+1-rem(hlength,2);

if (nargin == 1),
    t=1:xrow; h = tftb_window(hlength); trace=0;
elseif (nargin == 2)|(nargin == 3),
    h = tftb_window(hlength); trace=0;
elseif (nargin == 4),
    trace = 0;
end;

if (N<0),
    error('N must be greater than zero');
end;
[trow,tcol] = size(t);
if (xcol==0) | (xcol>2),
    error('X must have one or two columns');
elseif (trow~=1),
    error('T must only have one row');

```

```

elseif (2^nextpow2(N)~=N & nargin==5),
    fprintf('For a faster computation, N should be a power of two\n');
end;

[hrow,hcol]=size(h); Lh=(hrow-1)/2; h=h/h(Lh+1);
if (hcol~=1) | (rem(hrow,2)==0),
    error('H must be a smoothing window with odd length');
end;

tfr= zeros (N,tcol) ;
if trace, disp('Pseudo Wigner-ville distribution'); end;
for icol=1:tcol,
    ti= t(icol); taumax=min([ti-1,xrow-ti,round(N/2)-1,Lh]);
    tau=-taumax:taumax; indices= rem(N+tau,N)+1;
    tfr(indices,icol) = h(Lh+1+tau).*x(ti+tau,1).*conj(x(ti-tau,xcol));
    tau=round(N/2);
if (ti<=xrow-tau)&(ti>=tau+1)&(tau<=Lh),
    tfr(tau+1,icol) = 0.5 * (h(Lh+1+tau) * x(ti+tau,1) * conj(x(ti-tau,xcol))
+ ...
                                h(Lh+1-tau) * x(ti-tau,1) * conj(x(ti+tau,xcol)))
;
end;
if trace, disprog(icol,tcol,10); end;
end;

tfr= fft(tfr);
if (xcol==1), tfr=real(tfr); end ;

if (nargout==0),
    tfrqview(tfr,x,t,'tfrpwv',h);
elseif (nargout==3),
    f=(0.5*(0:N-1)/N)';
end;

```



```
    pi = input('Give me the probability of the intersection: ');
end

x = pi/pb; %conditional probability
i = input('Do you want to know if the events (sets) are independent? (y/n):
','s');
if i == 'y'
if pa == x
    disp('The events (sets) are independent.');
```

else

```
    disp('The events (sets) are not independent.');
```

end

```
else
end
end

return,
```